Materials Advances

Accepted Manuscript

This article can be cited before page numbers have been issued, to do this please use: R. Hossain, N. F. Materer and A. W. Apblett, *Mater. Adv.*, 2026, DOI: 10.1039/D6MA00700G.

ROYAL SOCIETY OF CHEMISTRY

rsc.li/materials-advances

View Article Online
DOI: 10.1039/D6MA00700G

Innovative Sensor Technologies for Trace Detection of Organic Peroxide Explosives and Industrial Hydroperoxides

Rayhan Hossain[1]*, Allen Apblett[2], and Nicholas F. Materer[2,]*

[1]Department of Natural Sciences, 107 Science Faculty Center, University of Michigan, Ann Arbor, Michigan 48109, USA
[2] Department of Chemistry, 316 Physical Science, Oklahoma State University, Stillwater, Oklahoma 74078, USA
* Correspondence: rhossain@umich.edu, nicholas.materer@okstate.edu

Abstract

Organic peroxide compounds such as triacetone triperoxide (TATP), hexamethylene triperoxide diamine (HMTD), tert-butyl hydroperoxide (TBHP), and cumene hydroperoxide (CHP) present significant analytical and safety challenges because of their instability, low vapor pressures, and hazardous oxidative behavior. In this work, titanium(IV)-based ionic liquid thin films containing trifluoromethanesulfonic acid were investigated as colorimetric sensing materials for vapor-phase peroxide detection under controlled laboratory conditions. The sensing platform exhibited observable and reproducible colorimetric responses toward peroxide vapors, with response kinetics strongly influenced by acid concentration and peroxide volatility. Silica-supported acidified films demonstrated enhanced sensitivity toward TATP vapor, exhibiting apparent first-order kinetic behavior and achieving a peroxide sensing equivalency of approximately 0.014 ppm under extended exposure conditions. In contrast, minimal response was observed for HMTD vapor, consistent with its significantly lower vapor pressure and reduced vapor-phase reactivity under identical experimental conditions. TBHP and CHP vapors also generated measurable colorimetric responses. A multi-modal analytical approach involving atomic force microscopy (AFM), Fourier-transform infrared spectroscopy (FTIR), X-ray photoelectron spectroscopy (XPS), gas chromatography-mass spectrometry (GC-MS), and ion mobility spectrometry (IMS) was employed to characterize the sensing films and validate peroxide interactions. These findings establish an acid-enhanced Ti(IV)-based thin-film platform for selective vapor-phase peroxide sensing and provide mechanistic insights relevant to future development of laboratory-scale colorimetric peroxide detection systems.

Keywords: titania; ionic liquid, organic peroxide vapor; thin film sensor; colorimetry

1. Introduction

Organic peroxide compounds continue to present major challenges in forensic science, industrial safety, environmental monitoring, and counterterrorism applications because of their high

View Article Online
DOI: 10.1039/D6MA00700G

energetic instability, oxidative reactivity, and potential misuse in improvised explosive devices (IEDs). Among these compounds, triacetone triperoxide (TATP) and hexamethylene triperoxide diamine (HMTD) have received substantial attention owing to their use in peroxide-based explosives and their extreme sensitivity to friction, impact, and thermal decomposition.

Organic peroxides have historically been exploited in the fabrication of improvised explosive devices (IEDs) for terrorist activities, making them a persistent concern for the scientific and security communities.[1-4] Despite their significance, the detection of organic peroxide vapors remains challenging due to their inherently low vapor pressure and limited reactivity. Various advanced analytical techniques, including mass spectrometry, ion-mobility spectrometry, and air sampling, have been explored for the detection of organic peroxide vapors.[5-11] However, these methods often require complex instrumentation and stringent operating parameters, which can limit their practical application. Despite extensive research, reliable vapor-phase detection of organic peroxides under ambient conditions remains an ongoing challenge.

Hydroperoxides such as TBHP, and CHP are widely used in industrial processes, including polymerization, oxidation reactions, and organic synthesis. However, their instability and potential to decompose violently pose significant safety risks, necessitating sensitive and reliable detection methods. Thin films composed of acidified titanyl-ionic liquid solutions provide an innovative approach to detecting these hydroperoxides through a distinct and rapid colorimetric response.[12-15] TBHP and CHP exhibit distinct colorimetric signatures due to their structural differences. TBHP, with its higher vapor pressure and branched alkyl structure, interacts more rapidly with the film, producing an immediate and intense color change. In contrast, CHP, which has a lower vapor pressure and an aromatic backbone, generates a slower but equally detectable response.[16-24] These differences suggest that the films could be fine-tuned to not only detect but also differentiate between specific hydroperoxides based on their vapor-phase behavior and reactivity. The versatility of these thin films allows their integration into portable detection systems for real-time monitoring of TBHP and CHP vapors in industrial environments. Moreover, their ability to provide a direct visual response without requiring complex instrumentation makes them uniquely suited for on-site applications, such as detecting explosive precursors or monitoring air quality in confined spaces. By leveraging the interplay between acid catalysis, ionic liquid stabilization, and colorimetric sensing, this novel detection method represents a transformative advancement in the safe and efficient monitoring of hydroperoxides.[25]

In recent years, triacetone triperoxide, one of the most hazardous primary explosives, has gained prominence in terrorist activities.[26-28] TATP is particularly challenging to detect due to its lack of fluorescence activity, absorbance of UV light, and poor ionization properties.[29-31] Conventional detection methods either rely on expensive instrumentation, require extensive sample preparation, or fail to identify TATP in the gas phase. We introduce a colorimetric sensing approach that exhibits reproducible vapor-phase responses to TATP under acidic conditions, with measurable intensity changes observed at low vapor pressures. This sensor identifies TATP vapor through its acidic decomposition products, such as H_2O_2, even at very low concentrations, with a corresponding to approximately 0.01% of its reported saturation vapor pressure. This achievement was facilitated by utilizing a liquid acid reagent for detection. The sensor successfully differentiates TATP and other chemical oxidants, including hexamethylene

View Article Online
DOI: 10.1039/D6MA00700G

triperoxide diamine, cumene hydroperoxide, tert-butyl hydroperoxide, bleach, and peracetic acid under controlled vapor-phase interferent screening conditions. No measurable response was observed under the specific laboratory conditions tested for common volatile interferents.

After optimizing and evaluating the sensitivity of cellulose and silicon-based test strips, both with and without acidic environments, for the detection of hydrogen peroxide vapors,[32] it was subsequently decided that these sensing materials could be used to detect vapors of organic peroxides such as TATP, HMTD, TBHP, and CHP.[33-35] However, the experimental results indicate that the detection of organic peroxide vapors poses significant challenges, primarily due to their inherently reduced reactivity and lower vapor pressure compared to hydrogen peroxide. Moreover, it is noteworthy that organic peroxides have historically been the principal constituent in the explosive charge mechanisms of improvised explosive devices (IEDs), underscoring their heightened safety risk. Silicon-based test strips exposed to excess acid concentration demonstrated the ability to detect TATP vapors over an extended detection period. In contrast, the same silicon-based sensing materials exhibited limited or no discernible response to HMTD vapors under identical exposure conditions and time intervals. This highlights the differential reactivity and vapor signatures of these compounds, posing distinct detection challenges for organic peroxides.

When titanyl-ionic liquid solutions incorporated into acid-based thin films were exposed to organic peroxides, they demonstrated limited sensitivity to organic peroxide vapors. Notably, a discernible color change required prolonged exposure, exceeding seven days. Recent findings suggest that these films are sensitive to hydrogen peroxide (H_2O_2), a byproduct of the reaction between TATP and acid.[36] To evaluate their potential for detecting organic peroxide vapors, various formulations of titanium(IV)-ionic liquid solutions with excess acid concentrations were prepared. Among these, titanium(IV) oxysulfate in trifluoromethanesulfonic acid, detailed in the experimental section, exhibited enhanced performance. Films derived from these solutions displayed significantly improved sensitivity to TATP vapor ($P_{vapor} \sim 10^{-2}$ torr at 25 °C). However, detection of HMTD vapor remained challenging due to its substantially lower vapor pressure ($P_{vapor} \sim 10^{-4}$ torr at 25 °C). To further optimize the films, titanyl sulfate-based coatings were developed on silicon substrates, employing an ionic liquid solvent instead of isopropanol.[37-38] Sulfuric acid and trifluoromethanesulfonic acid were utilized as acid components. The inclusion of the ionic liquid effectively prevented desiccation, preserving the acidic environment and extending the functional lifetime of the films. Among the variations, trifluoromethanesulfonic acid-based films demonstrated superior sensitivity to organic peroxides, comparable to previous studies. Importantly, these films exhibited enhanced long-term stability, establishing them as the most effective and durable formulation for detecting organic peroxide vapors, with the ionic liquid.

The development of a detection method based on perceptible colorimetric changes offers a promising alternative. Such an approach has the potential to provide a straightforward and effective means of identifying the presence of organic peroxides, enhancing both practicality and accessibility in field applications. The detection of peroxide vapors using this method could be a valuable advance for the presence of these peroxides through color change.

Safety Warning: Organic peroxide compounds such as TATP and HMTD are highly energetic

View Article Online
DOI: 10.1039/D6MA00700G

primary explosives and present significant risks of thermal instability, friction sensitivity, and shock-induced decomposition. All syntheses and handling procedures involving peroxide explosives were performed on milligram-scale quantities using appropriate personal protective equipment inside a ventilated fume hood equipped with blast shielding. All experimental procedures complied with institutional laboratory safety regulations and hazardous materials handlingprotocols.

2. Experimental Details

2.1. Preparation of Titanyl-Ionic Liquid Solution with Acid

Titanium(IV) oxysulfate-based ionic liquid solutions were prepared by dissolving 1.69 g of deionized water with 0.58 g of trifluoromethanesulfonic acid under gentle heating. Subsequently, 0.5 g of titanium(IV) oxysulfate hydrate ($TiOSO_4 \cdot xH_2O$) was added, and the mixture was heated in a boiling water bath for 5 minutes until a clear solution was obtained. After cooling to room temperature, the solution was filtered through a 0.20 μm syringe filter to remove suspended particulates. Finally, 0.81 g of 1-ethyl-3-methylimidazolium hydrogen sulfate was added and mixed thoroughly to obtain a homogeneous ionic-liquid-based solution. The solution was stored under inert atmosphere prior to use.
A 20 μL aliquot of the prepared titanyl–ionic liquid solution was carefully dispensed onto the silica substrate to form a thin film. The volume was not further adjusted after deposition to fit the boxes on the pad and a nice thin film was prepared. Then the thin film was placed in the experimental setup which was in the expose chamber of the experimental setup and the sample was exposed at different concentrations of organic peroxide vapor. The total concentration of organic peroxide vapor was measured in the ppm range by measuring the absorbance of the colored solution into bubbler (E) of the experimental setup. For solid peroxide exposures, vapor concentrations were not directly quantified; instead, response behavior was compared using peroxide sensing equivalency relative to hydrogen peroxide calibration.

2.2. Preparation of Titanyl-Ionic Liquid Solution with Excess Acid

The same procedure was used for the preparation of Titanyl-Ionic Liquid Solution with excess acid except there was excess trifluoromethanesulfonic acid was taken in the test tube.

2.3. High Acid Content Films Testing Setup and Methodology

View Article Online
DOI: 10.1039/D6MA00700G

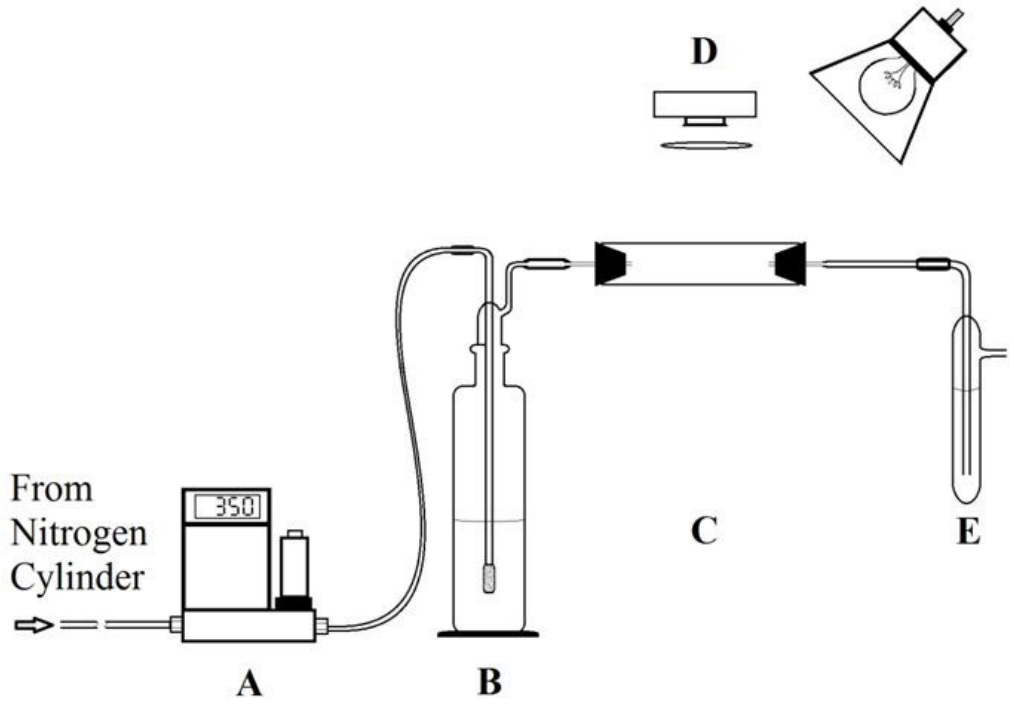

Figure 1. Schematic diagram of the peroxide exposure apparatus that depicts the (A) flow controller, (B) bubbler to entrain the peroxide vapor, (C) exposure chamber, (D) detection system, and (E) a bubbler used to determine the total concentration of peroxide in the flow. No direct gas-phase concentration measurement was performed for solid peroxide samples.

A schematic diagram of the experimental apparatus setup utilized to expose and track the thin films is shown in Figure 1. Peroxide quantification and intensity measurements were carried out along with the preparation of the detection solution and exposure apparatus. The only two differences between these exposures were the removal of the apparatus's gas flow and the addition of solid TATP and HMTD samples to the PTFE cell compared to liquid TBHP, and CHP. In order to expose the material, 0.10 g of solid TATP or HMTD was weighed and positioned in the PTFE cell placed inside the exposure chamber about 2 cm away from the thin films that were already present on the silicon substrate. A 20 W incandescent light was placed over the PTFE cell to deliver identical lighting for the slide along with a Logitech Pro 9000 USB camera filmed images of the sample throughout introduction to peroxide vapor. Exposures were prolonged to 4 days to ensure high vapor diffusion throughout the cell since the silicon test strip surface was exposed by the evolution and diffusion of vapor from the solid peroxides. There was no attempt to quantify the concentrations of organic peroxide in the gas phase. But the previous measurements of the corresponding gaseous hydrogen peroxide sensitivities were directly compared to the sensitivities of the high acid content films to gaseous organic peroxides. The peroxide sensing equivalency is the term used to describe this idea; the greater the number, the more sensitive the film is to organic peroxide vapor. All the images were analyzed using the ImageJ software (version 1.53k, 2021), available from the National Institutes of Health at https://imagej.nih.gov/ij/, in order to plot an intensity vs. time plot.

2.4. Preparation of Titanium (IV) Oxysulfate and peroxide Solution

2.4.1. Titanium (IV) oxysulfate stock solution

View Article Online
DOI: 10.1039/D6MA00700G

The peroxide vapor concentration was measured through a so-called colorimetric procedure formed by OSHA. This method requires the preparation of titanium (IV) oxysulfate stock solution in sulfuric acid. At first in a beaker 5.5 g of dried $TiOSO_4{\cdot}xH_2O$ (Strem Chemicals) was taken and then 20 g of ammonium sulfate (Spectrum, A.C.S. Reagent) was mixed in the beaker with a heated solution of 100 mL of concentrated sulfuric acid (Pharmco-Aaper, A.C.S. Reagent). The mixture was heated to dissolve all the chemicals. Then the mixture was cooled to room temperature, after cooling, 350 mL of nano pure water was added in the resulting solution. A 0.40 µm filter paper was used to remove any suspended particles, and then finally more nano pure water was added to further dilute the titanium(IV) oxysulfate solution to make the total volume of the stock solution 500 mL. Titanium reagent, commonly referred to as collecting solution, is this stock solution diluted to 1:50.

2.4.2. Peroxide stock solution

TATP and HMTD solid samples were synthesized by Dr. Hossain. However, liquid samples of cumene hydroperoxide, tert-butyl hydroperoxide were bought from sigma aldrich chemicals and used as received (80 wt% and 70 wt%, respectively, as specified by the manufacturer). At first 16.85 µL of cumene hydroperoxide was taken in a 100 mL volumetric flask and then distill water was added to fill up the flask up to the mark. This is the required cumene hydroperoxide stock solution, aliquot of this stock solution was used as standard. This stock solution was used for the preparation of series of standard solutions in the range of 7 to 140 µg/mL. Similarly, for tert-butyl hydroperoxide, 2.14 µL of the commercial solution was used directly in our experiments. While a full stock solution was not prepared for TBHP as it was used at lower levels, the volume was carefully measured and appropriately diluted within the working matrix as needed.

2.4.3. Analysis of samples and Standards

Standard hydroperoxide solutions were made by placing 5 mL of titanium reagent in each of 6 vials and then aliquots of the standard hydroperoxide solutions were added. The total volume was adjusted to 15 mL with nano pure water. The absorbance of each sample solution, blank and standard were determined at 410 nm with 100 cary UV-Vis spectrophotometer. 0.00 absorbance was measured for the reagent blank. After that, a standard calibration curve was plotted from the obtained absorbance values of the standard hydroperoxide solutions. This standard curve should go through the origin.

2.4.4. Analysis of the slope with hydrogen peroxide slope

To assess whether the response behavior toward different hydroperoxides differed significantly, calibration slopes obtained using titanium reagent were statistically compared using a two-slope t-test. The resulting slope for cumene hydroperoxide calibration curve is $6.1 \pm 0.3 \times 10^{-3}$ from Figure 2. The resulting slope for hydrogen peroxide calibration curve is $1.78 \pm 0.3 \times 10^{-2}$. In fact, the slope of the regression line for cumene hydroperoxide is 6.1×10^{-3} and the slope for hydrogen peroxide is 1.78×10^{-2}. This difference was evaluated using a two-slope t-test.
To compare the similarity of the slopes, a p-value approach was used. A probability value of less than 0.05 indicates that the two slopes are significantly different from each other. The t-value is calculated using the following equation.

$$t = \frac{b_1 - b_2}{\sqrt{s_{b_1}^2 + s_{b_2}^2}}$$

From the calculation, t-Value= 27.6
Degrees of freedom= 11

View Article Online
DOI: 10.1039/D6MA00700G

Probability= 0.0

(A)

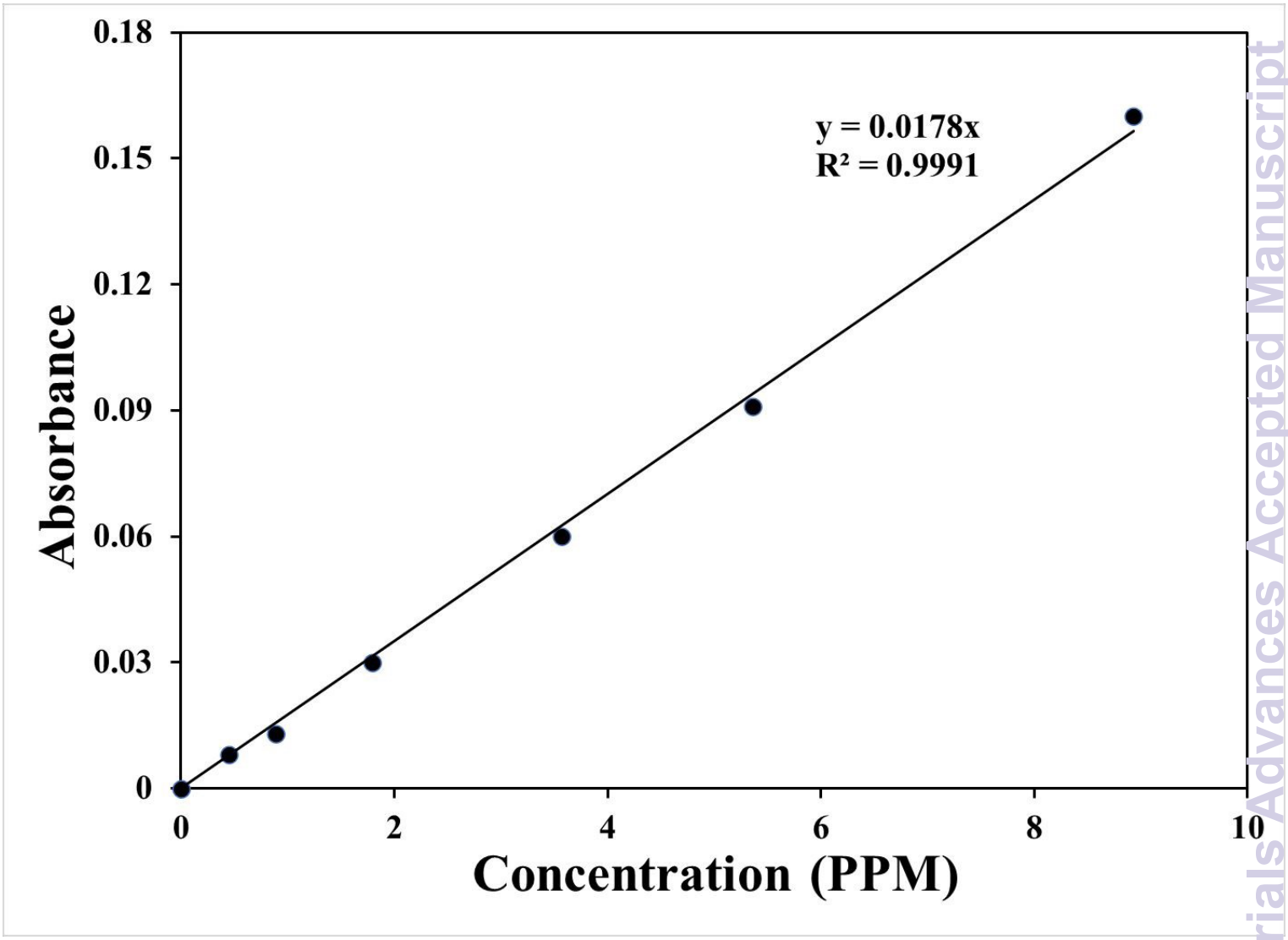

View Article Online
DOI: 10.1039/D6MA00700G

(B)

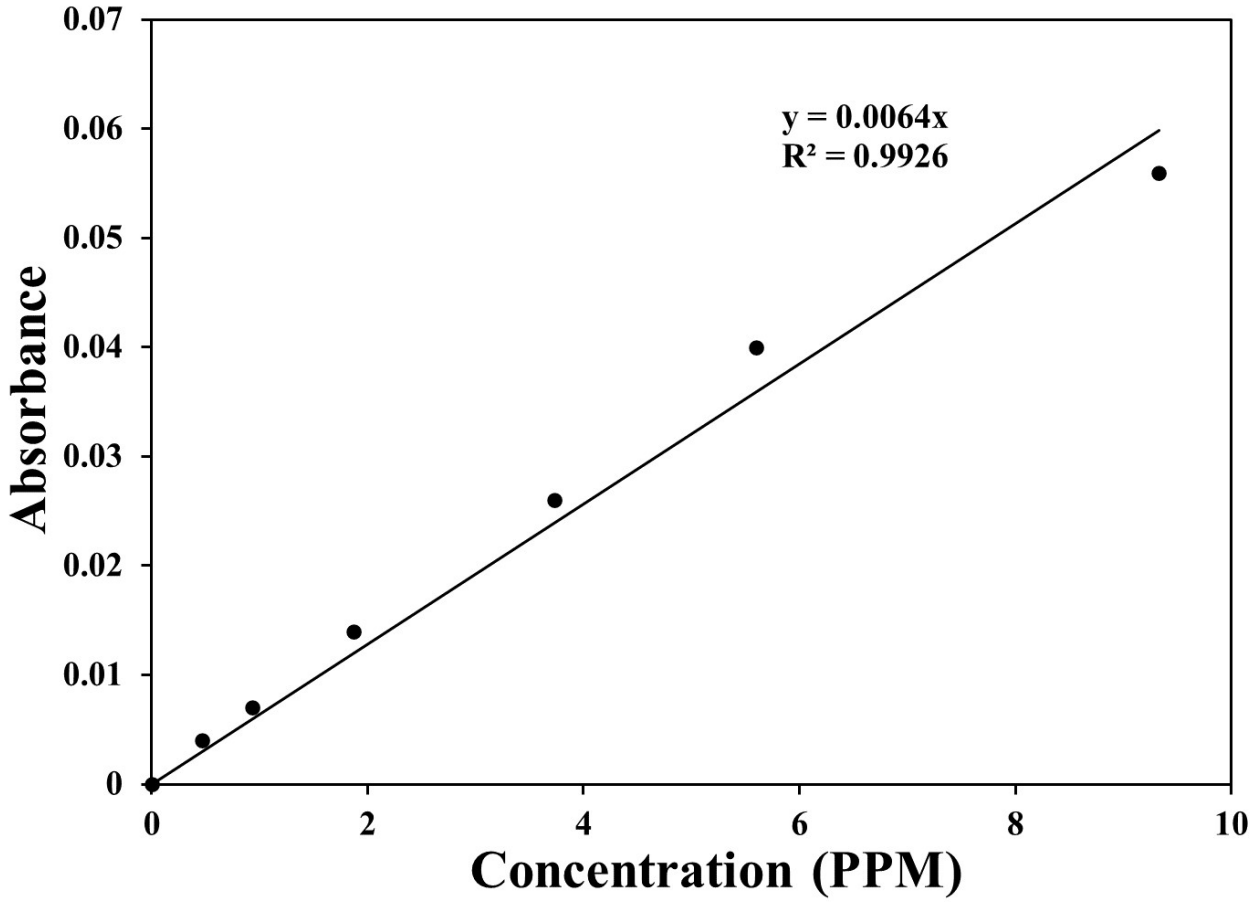

Figure 2. Calibration curves for hydroperoxide standards. (A) Hydrogen peroxide showing linear response ($R^2 = 0.9991$) with zero-intercept fitting. (B) Cumene hydroperoxide calibration curve showing excellent linearity ($R^2 = 0.9926$) with zero-intercept fitting.

In this case the p-value is < 0.00001, which is less than 0.05 indicates that the two slopes are significantly different from each other.

2.4.5. Analysis of the slope with cumene hydroperoxide slope

The resulting slope for tert-butyl hydroperoxide calibration curve is $5.4 \pm 0.2 \times 10^{-3}$ from Figure 3. The resulting slope for cumene hydroperoxide calibration curve is $6.1 \pm 0.3 \times 10^{-3}$ from Figure 2. In fact, as can be seen from both Figure, the slope of the regression line for cumene hydroperoxide is 6.1×10^{-3} and the slope for tert-butyl hydroperoxide is 5.4×10^{-3}. This difference was evaluated using a two-slope t-test.

View Article Online
DOI: 10.1039/D6MA00700G

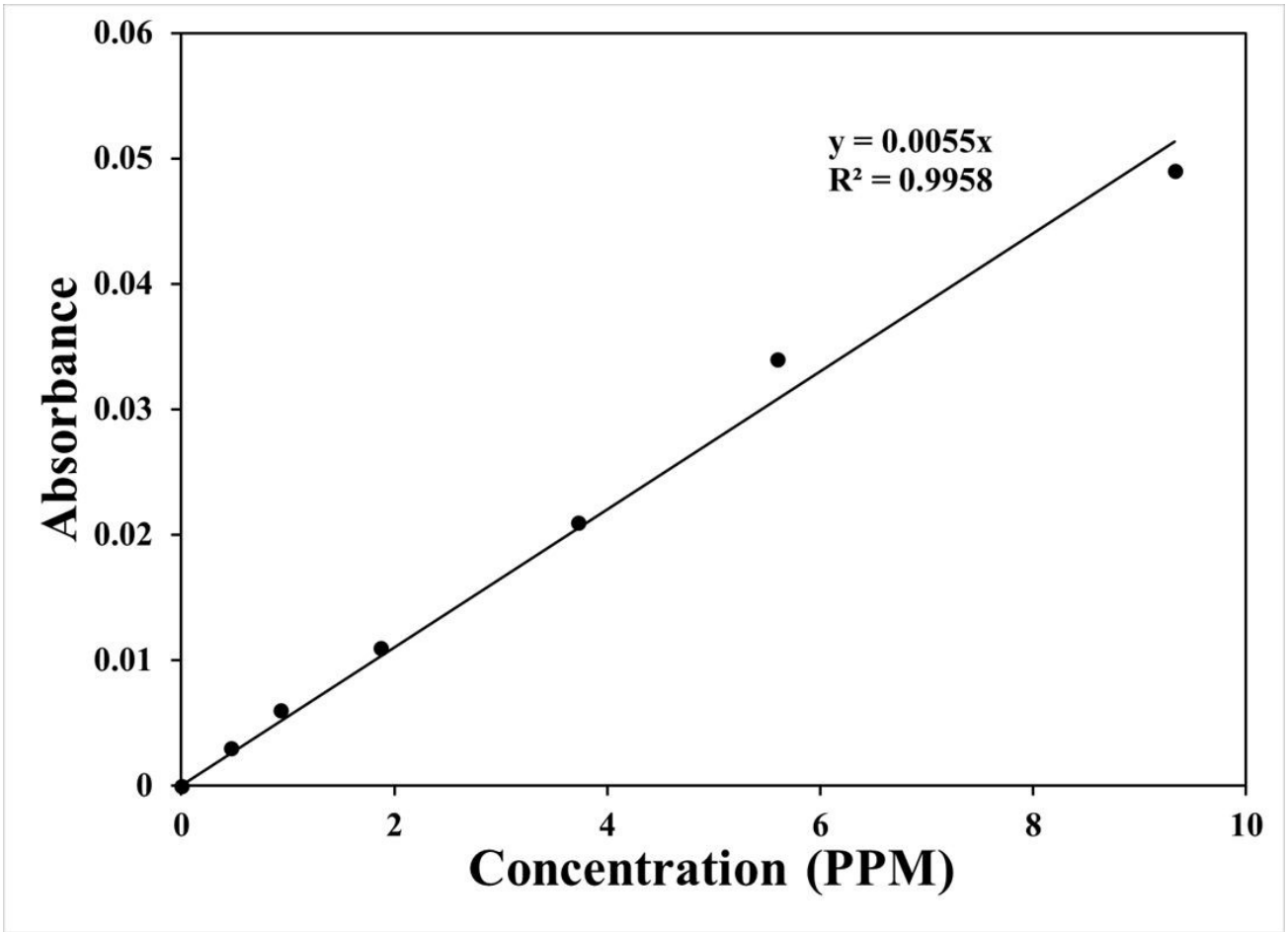

Figure 3. Calibration curve for the different concentration of standard tert-butyl hydroperoxide solution. The calibration was extremely linear ($R^2 = 0.9958$), and the zero-intercept is set.

A probability value of less than 0.05 indicates that the two slopes are significantly different from each other.
From the calculation, t-Value= 1.69
Degrees of freedom= 10
Probability= 0.121
In this case the p-value is 0.121, which is greater than 0.05 indicates that there is no significant difference between them.

2.4.6. Equipment Used

In the beginning, cellulose was used to make test strips, giving the solution and peroxides a vast surface area to react on. The inclusion of a strong acid is suggested in this work because the rate of reaction was not very high. The test strips made of cellulose were destroyed (became a dark shade of black) when the strong acid, trifluoromethanesulfonic acid was added. As a result, it is proposed that silica strips purchased for Thin Layer Chromatography be used. These strips are simple to use, consistently produced strips, and are not decomposed by strong acid. We utilized Baker-Flex TLC strips.

View Article Online
DOI: 10.1039/D6MA00700G

To construct a pad that was 5mm x 5mm in size, a 2-3 mm silica strip was first removed before the purchased strips were sliced into smaller test strips that were 5 mm wide. This silica pad's size was intended to closely resemble widely available Titanium (IV)-based cellulose test strips, which would be used to compare the reaction rates. To make sure that the silica was not creating any changes in the intensity, the extra silica beyond the 2-3 mm removal region would be used as a blank for intensity readings. When the light source changed during an experiment, the blank silica surface also made it possible to recalibrate the intensity values.

2.4.7. Instrumentation

All analytical measurements were carried out using standard characterization tools with detailed specifications as follows:

Gas Chromatography–Mass Spectrometry (GC–MS): Agilent 7890B GC system coupled with an Agilent 5977A Mass Selective Detector was used to analyze peroxide vapor samples. Separation was achieved using an HP-5ms capillary column (30 m × 0.25 mm × 0.25 μm film thickness). Helium was used as the carrier gas with a constant flow rate of 1 mL/min. The analysis was performed using a full-scan mass spectrometric method over an m/z range of 50–500, with splitless injection.

Ion Mobility Spectrometry (IMS): A handheld IMS detector (FLIR Systems, Model Fido X3) was used for field-detection and real-time monitoring of peroxide vapors.

Fourier-Transform Infrared Spectroscopy (FTIR): Spectra were recorded using a Bruker Alpha II FTIR spectrometer equipped with an attenuated total reflectance (ATR) module. The scan range was 4000–400 cm^{-1} with a resolution of 4 cm^{-1}. All measurements were performed under standard instrument calibration conditions.

X-ray Photoelectron Spectroscopy (XPS): Surface elemental analysis was performed using a Kratos AXIS Supra XPS system with a monochromatic Al Kα radiation source (1486.6 eV). Survey and high-resolution spectra were collected under ultrahigh vacuum conditions.

Atomic Force Microscopy (AFM): Surface topography was examined using a Bruker Dimension Icon AFM operated in tapping mode with silicon cantilevers (nominal tip radius ~8 nm).

UV–Visible Spectroscopy: A Cary 100 UV–Vis spectrophotometer (Agilent Technologies) was employed to generate calibration curves for quantification of hydrogen peroxide and organic peroxide vapors.

All instruments were operated according to the manufacturers' standard protocols, and calibration was conducted prior to each experimental session to ensure data reliability and reproducibility.

3. Results and Discussions

The interaction of titanium (IV) oxysulfate, an ionic liquid, and an acid catalyst at the microstructural level involves intricate molecular arrangements and dynamic interactions, creating a highly organized and reactive environment is shown in Figure 4. Titanium (IV) oxysulfate serves as the primary inorganic framework, forming a matrix that facilitates catalytic activity. The ionic liquid, acting as both a stabilizing medium and a hydration source, contributes to the structural integrity and maintains the film's dynamic functionality by modulating the physicochemical environment. The acid catalyst, such as trifluoromethanesulfonic acid, enhances the reactivity within this system by protonating reactive intermediates and accelerating oxidative decomposition processes. Together, these components establish a synergistic network, where the ionic liquid ensures mobility and stability, while the acidic environment amplifies reactivity. This molecular-level interplay highlights the system's sensitivity and selectivity for

View Article Online
DOI: 10.1039/D6MA00700G

organic and hydroperoxide detection, offering a robust and tunable platform for real-time chemical sensing. Here's a detailed visualization showing the interaction of titanium (IV) oxysulfate, ionic liquid, and an acid catalyst at the microstructural level with molecular arrangements and dynamic interactions.

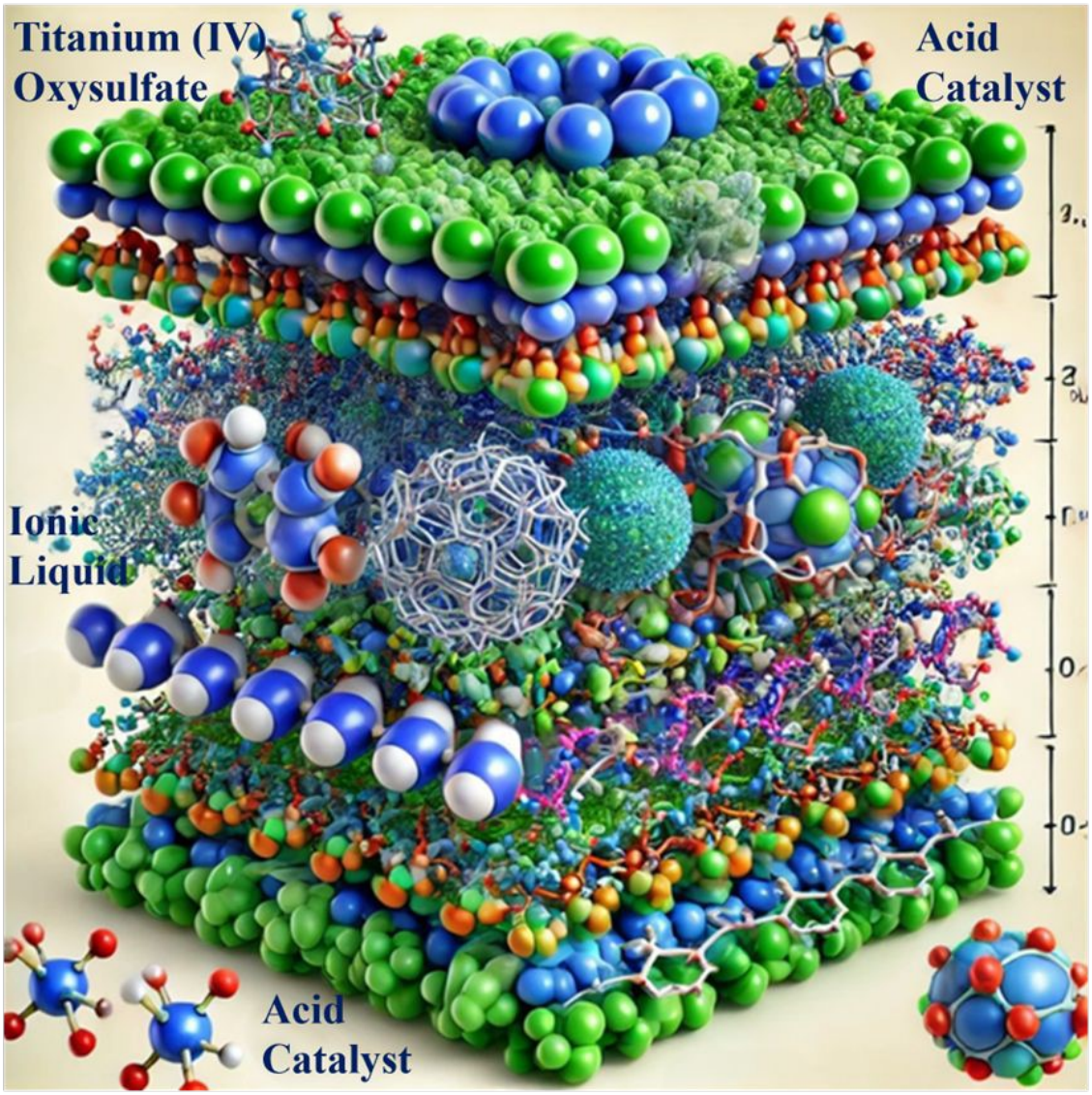

View Article Online
DOI: 10.1039/D6MA00700G

Figure 4. Visualization shows the interaction of Ti(IV) oxysulfate, ionic liquids, and an acid catalyst at the microstructural level.

Atomic force microscopy (AFM) was utilized to thoroughly evaluate the surface roughness of the prepared titania-based films, providing critical information about their microstructural characteristics and overall morphology. A film composed of 30 mass percent titania loading was carefully deposited onto a glass slide, and a 10 μm × 10 μm region of its surface was selected and analyzed to ensure localized characterization of the film's topography (see Figure 5). The root mean square roughness (Rq) of the measured area was determined to be 5.23 nm, which provides quantitative evidence of the film's surface morphology. This value indicates that the titania films exhibit a moderately smooth surface, showing uniformity at the nanometer scale without extreme topographical variations.

For comparison, the Rq value of Si(100) surfaces that have been etched using the RCA cleaning method an established technique for preparing clean, planar silicon surfaces for applications in microelectronics is remarkably low at 0.09 nm, reflecting their near-ideal flatness and minimal surface roughness.[39-40] At the other extreme, superhydrophobic films of trimethylsilanized silica using the sol-gel process exhibit Rq values close to 30 nm, signifying large peak-to-valley features. These topographical features are responsible for creating hydrophobicity by trapping air and reducing the interaction between water molecules and the surface.

View Article Online
DOI: 10.1039/D6MA00700G

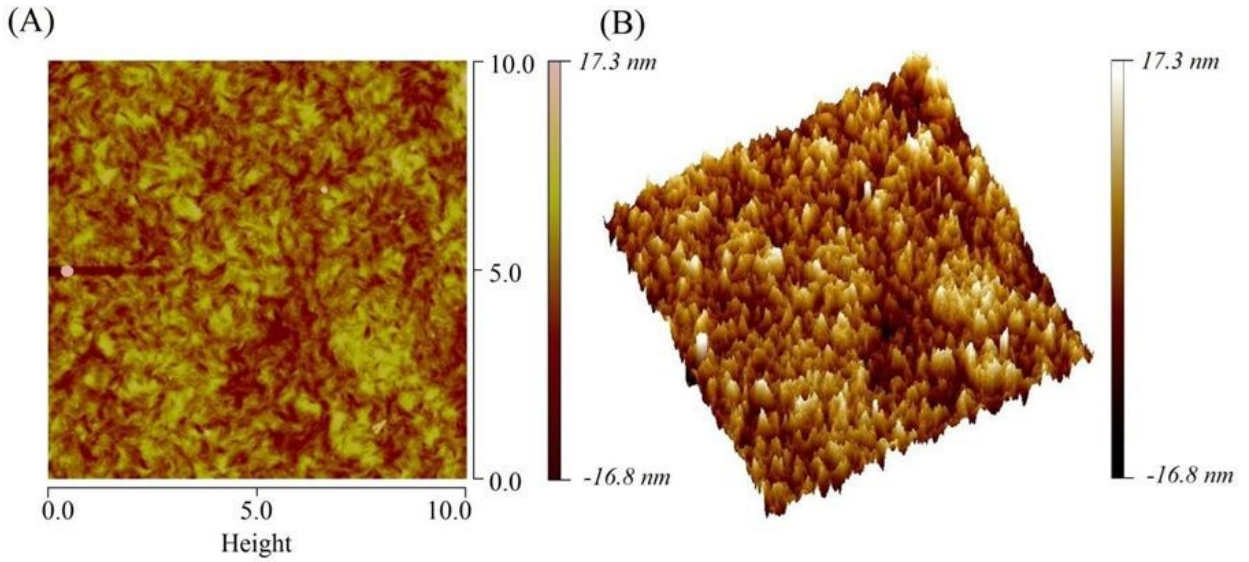

Figure 5. False-color images of (A) the height and (B) surface roughness of a titania-cellulose film, measured by AFM.

The moderate roughness likely results from the interplay between the slow evaporation rate of the solvent used during film preparation and the congealing behavior of the substrate matrix. These factors influence the structural assembly of the titania particles and the organization of the film as it forms, ultimately dictating the microstructural characteristics observed. This degree of roughness suggests that the films are sufficiently smooth for most sensing applications while maintaining structural features that ensure functional stability and interaction with target analytes. This unique balance between smoothness and topographical variability allows the films to function effectively as sensitive detection platforms while remaining stable and robust in a variety of operational conditions.

Thin Film's Reactivity to Organic Peroxides

When exposed to peroxide vapors, the films exhibit a discernible colorimetric response, consistent with prior observations from the analyzed films and test strips. The titania solution incorporating trifluoromethanesulfonic acid exhibited the characteristic yellow color shift upon exposure to TATP vapors. In contrast, films prepared with an excess of trifluoromethanesulfonic acid underwent a more pronounced transition to an intense shade of orange under identical conditions. However, exposure to HMTD vapors elicited only a faint color change in the excessively acidic films, while the less acidic films displayed no perceptible chromatic response.

TATP and HMTD Reaction Kinetics with the Acidic films

There was no color change when a controlled thin film was exposed to organic peroxide vapors without adding any titania. Similarly, for H_2O_2 experiments, the image series captured under controlled conditions were analyzed using ImageJ to quantify intensity as a function of exposure duration. Utilizing ImageJ software, reflection images were extracted from the dynamic red regions of the thin films, as illustrated in Figure 6.

View Article Online
DOI: 10.1039/D6MA00700G

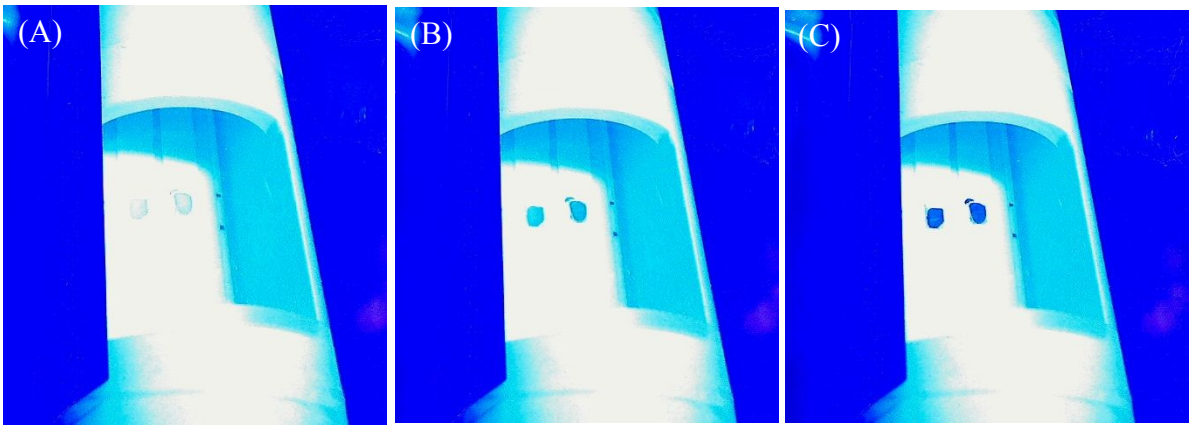

Figure 6. Progression of test strip color change during exposure to TATP vapors.

Applying the same techniques that we used within the enclosed box, the experiment was conducted within a PTFE cell. The corresponding images, captured using test strips placed within the PTFE cell under a blue light filter to enhance intensity resolution. Image A represents the initial exposure to peroxide vapors, Image B corresponds to the intermediate stage of the experiment, and Image C illustrates the final image post-exposure.

Figure 7 illustrates the normalized reflected intensity of the entire film as a function of exposure duration. It is evident that exposure of the films to TATP vapors in the presence of excess trifluoromethanesulfonic acid induces substantial alterations in intensity, resulting in a distinct colorimetric change. The excess trifluoromethylsulfonic acid film changes color in a manner that is consistent with apparent first-order behavior under the tested conditions. In contrast, films prepared under similar conditions exhibit negligible or no color change upon exposure to HMTD vapors, suggesting that the acidic film demonstrates first-order kinetics exclusively in the presence of TATP and remains non-reactive towards HMTD. Extended exposure times were required due to low vapor pressure and diffusion-limited transport of peroxide vapors within the sealed PTFE chamber.

View Article Online
DOI: 10.1039/D6MA00700G

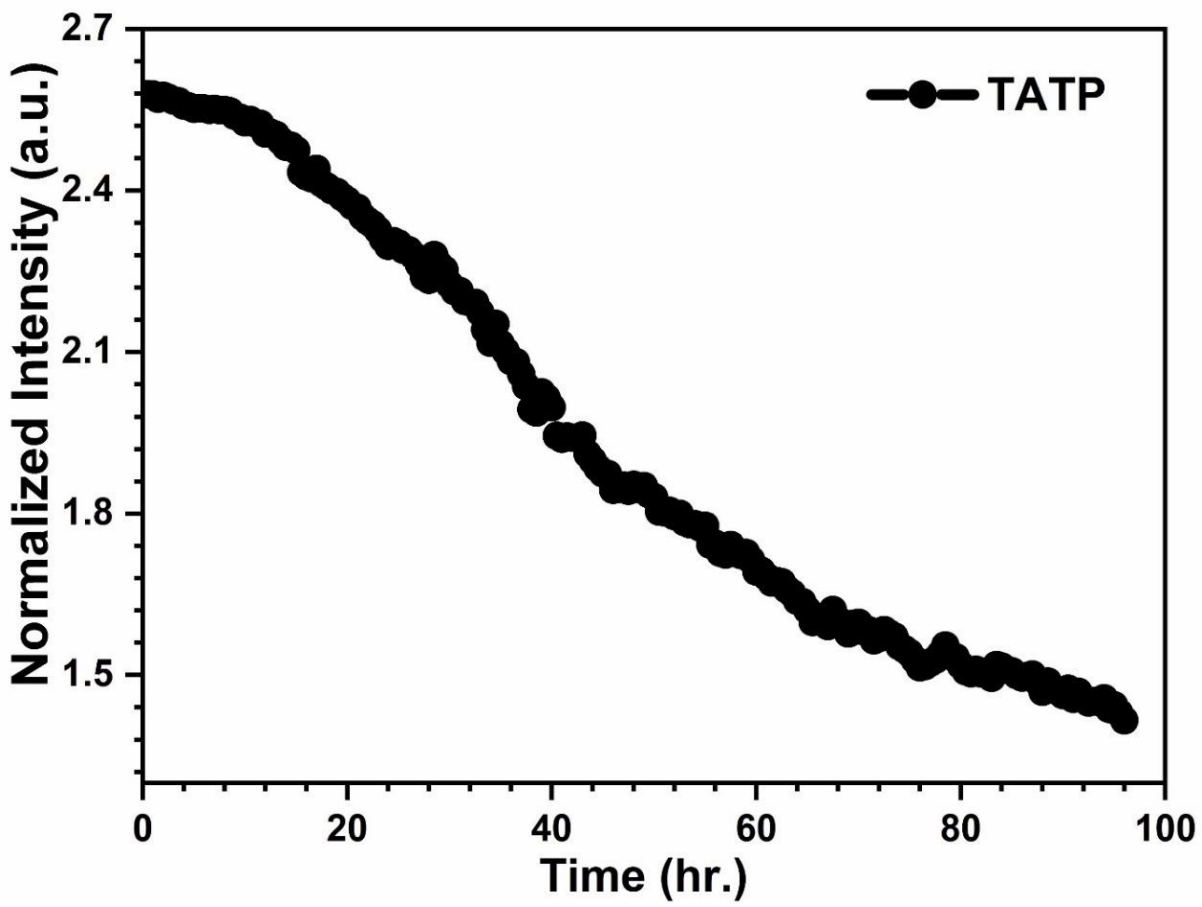

Figure 7. Plot showing the change in signal intensity over time for a silica test strip pre-treated with acid and subjected to TATP vapor exposure.

A reduction in reflected intensity, as depicted in Figure 7, is observed with increasing exposure time for the test strip subjected to excess acidification. Upon exposure to peroxide vapor, the intensity exhibits an exponential decline over time. The excess acidified test strips consistently demonstrate first-order kinetic behavior in response to TATP vapor diffusion, with a peroxide sensing equivalency of 0.014 ppm. Furthermore, a series of experimental runs with varying peroxide concentrations have been conducted to further validate this kinetic behavior.

Tert-butyl hydroperoxide Reaction Kinetics with the Acidic films

The experimental data presented in Figure 8 depict the response of a test strip exposed to a vapor phase concentration of 4.97 ppm of tert-butyl hydroperoxide over a 3-hour duration. Notably, a significant decrease in reflected intensity is observed as a function of exposure time, particularly for the acidified test strip variant. This attenuation in reflected intensity exhibits an exponential decay profile, characteristic of the interaction between the test strip surface materials and the hydroperoxide vapor.

In addition, a series of experimental runs were conducted across a range of TBHP concentrations, further investigating the concentration-dependent dynamics of the reflected intensity over time. The results from these varied conditions corroborate the observed trend, providing a comprehensive understanding of how

View Article Online
DOI: 10.1039/D6MA00700G

increasing hydroperoxide exposure correlates with a more pronounced reduction in reflected intensity, thereby highlighting the sensitivity of the test strip to different levels of TBHP vapor.

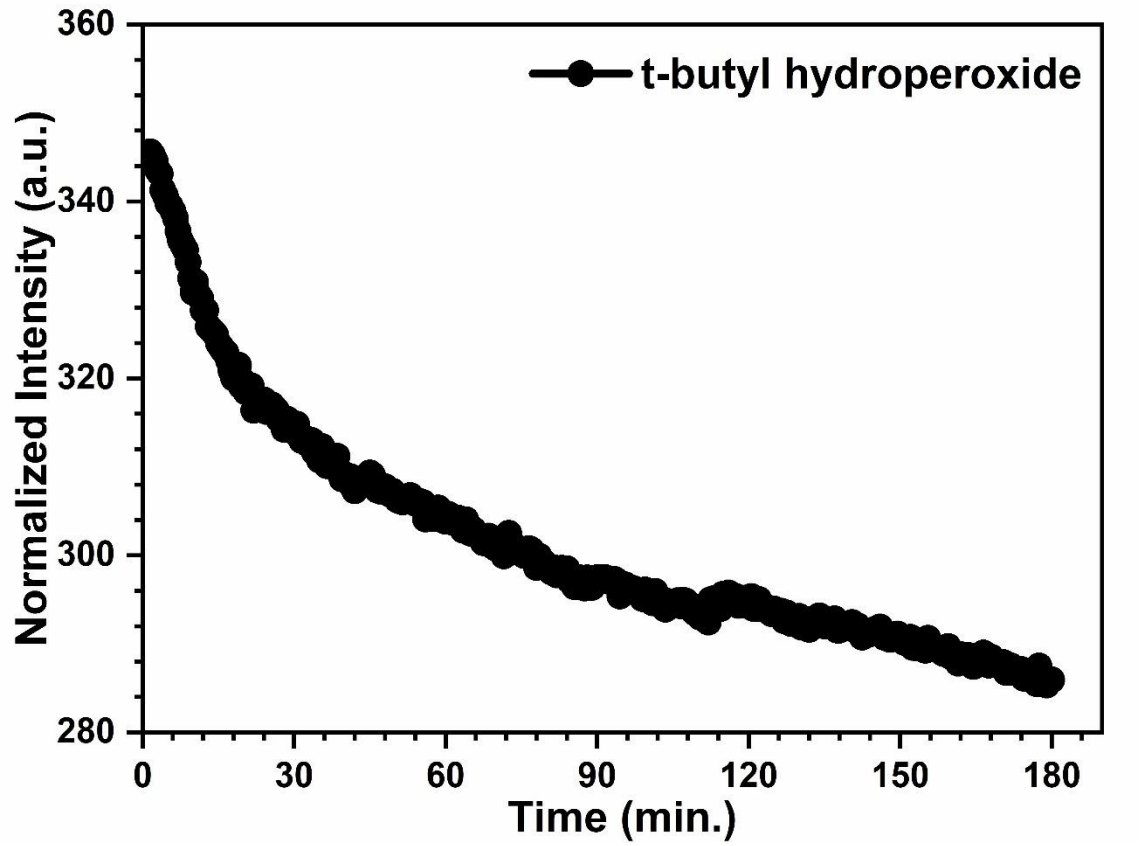

View Article Online
DOI: 10.1039/D6MA00700G

Figure 8. Intensity versus exposure time for a silica test strip – with acid, silica test strip was exposed to tert-butyl hydroperoxide concentration of 4.97 ppm for 3 hours.

The intensity versus exposure time plot conclusively demonstrates that the system follows first-order kinetic behavior following exposure to tert-butyl hydroperoxide vapor. This was confirmed by the application of the rate constant equation, where the resulting negative slope of the plot corresponds to the characteristic exponential decay associated with first-order reactions. Linear regression analysis of the data further substantiates this observation, yielding a precise mathematical representation of the kinetic behavior.

As exposure time progresses, a saturation point is reached, at which the reflected intensity plateaus. When saturation occurs the reflected intensity also stops as there were no active titania materials remaining to interact with tert-butyl hydroperoxide vapor. Once this saturation threshold is achieved, no additional chemical interaction occurs, effectively halting the intensity change. Additionally, under excess acidic conditions, the test strips exhibit clear first-order kinetic behavior in the presence of diffusing TBHP vapor. The peroxide sensing equivalency of the system was quantified, revealing a corresponding to a peroxide sensing equivalency of approximately 0.09 ppm of TBHP, which reflects the system's sensitivity and its potential for precise quantification of peroxide vapor concentrations in real-world applications.

Cumene hydroperoxide Reaction Kinetics with the Acidic films

The experimental data presented herein pertains to the exposure of test strips to 3.37 ppm of cumene hydroperoxide vapor over a 3-hour duration. As illustrated in Figure 9, a decrease in reflected intensity is observed in the acidified test strips as exposure time increases. This attenuation of reflectance follows an exponential decay pattern, indicative of the interaction between the hydroperoxide vapor and the surface materials.

Additional experimental runs were conducted across varying concentrations of cumene hydroperoxide to further elucidate the concentration-dependent behavior of this phenomenon. These results consistently demonstrate an exponential decline in reflected intensity, which appears to be a characteristic response of the test strip under exposure to hydroperoxide vapors.

View Article Online
DOI: 10.1039/D6MA00700G

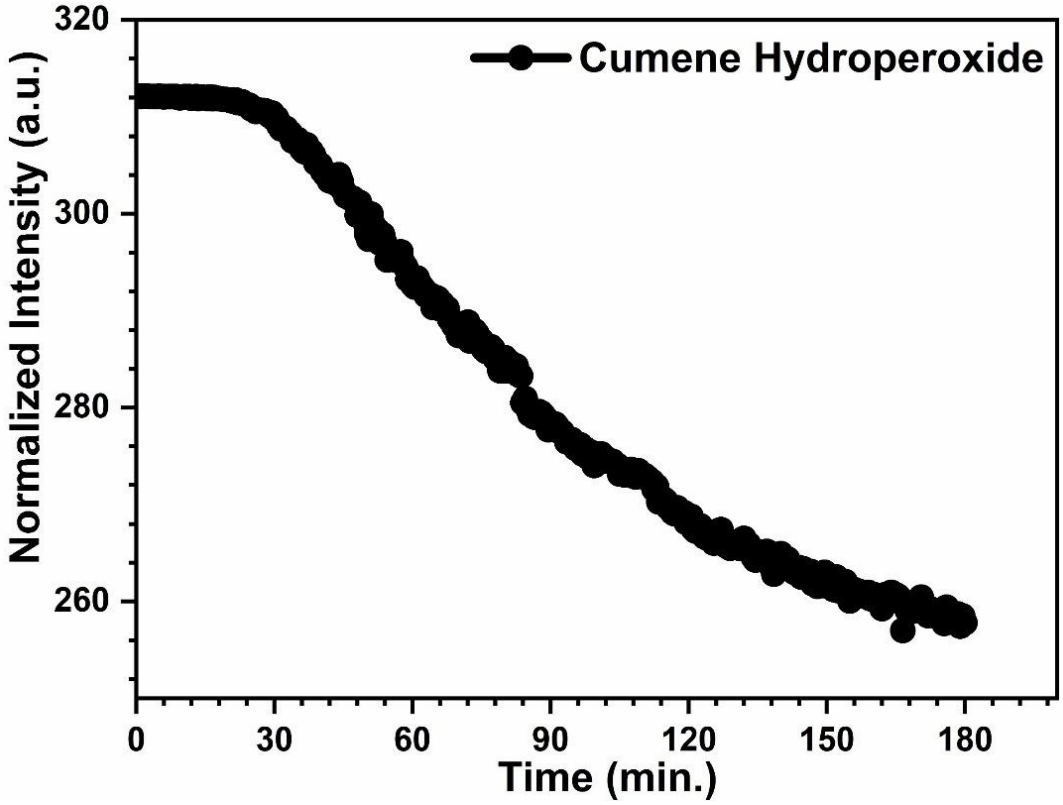

Figure 9. Intensity versus exposure time for a silica test strip – with acid, silica test strip was exposed to cumene hydroperoxide concentration of 3.37 ppm for 3 hours.

The intensity versus exposure time plot unequivocally demonstrated first-order kinetic behavior following exposure to cumene hydroperoxide vapor. The observed data were consistent with an exponential decay in reflected intensity. By applying the rate constant equation to the experimental data, a negative slope was derived, confirming the rate of intensity reduction as a function of time. Additionally, linear regression analysis of the intensity-time plot yielded a high degree of correlation, further supporting the first-order kinetics of the system.

At longer exposure times, the system reached a saturation point, where the reflected intensity plateaued. This cessation of intensity change is attributed to the depletion of active titania sites on the test strip, which are no longer available to interact with the diffusing CHP vapor. As a result, no further reaction occurs once the available active sites are no longer available, leading to a stabilization of the reflected intensity. Moreover, under conditions of excess acidic test strips, the observed first-order kinetic behavior was maintained across a range of CHP vapor concentrations. The peroxide sensing equivalency was determined to be 0.07 ppm, establishing the sensitivity of the test strips to low concentrations of cumene hydroperoxide vapor. This finding is significant for the application of such test strips in environments requiring precise detection of peroxide levels, where the kinetics of peroxide interaction with the sensor material provide a reliable measure of vapor concentration.

View Article Online
DOI: 10.1039/D6MA00700G

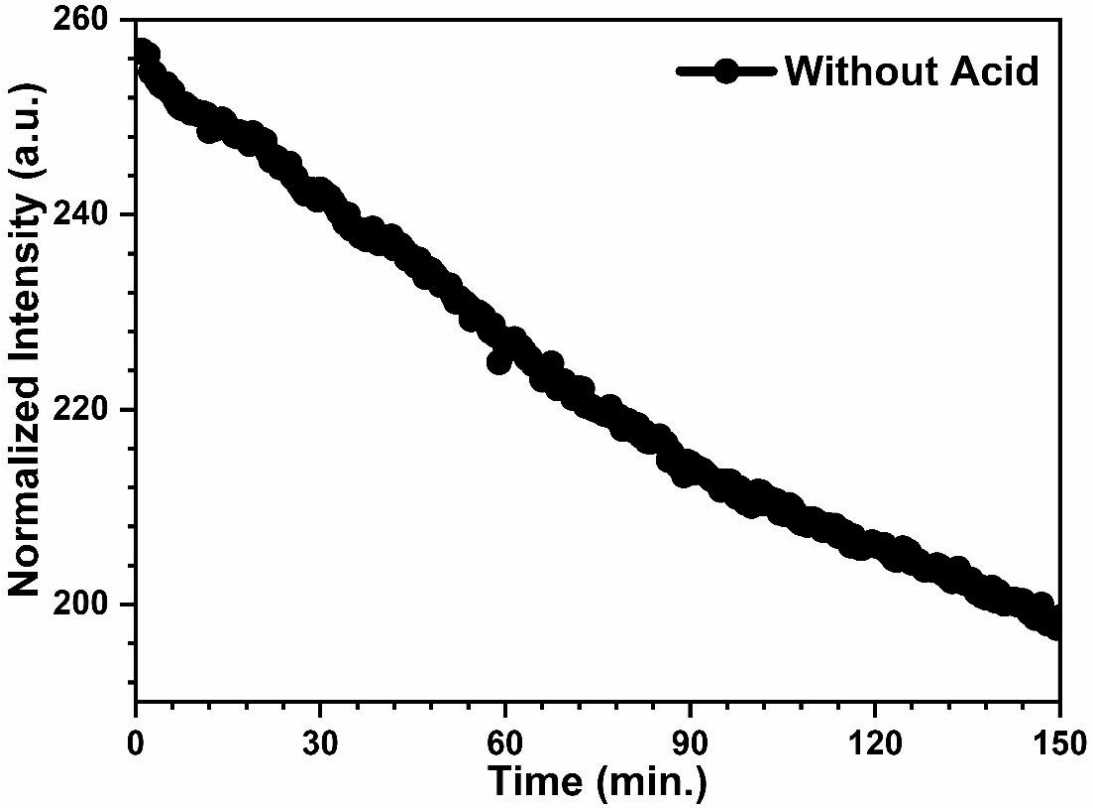

Figure 10. Intensity versus exposure time for a silica test strip – without acid, silica test strip was exposed to cumene hydroperoxide concentration of 1.22 ppm for 2.5 hours.

The intensity versus exposure time plot for cumene hydroperoxide vapor exposure on a silica-based test strip without acidic film is presented in Figure 10. Analysis of the data reveals that the system exhibits zero-order kinetic behavior under these conditions. Unlike first-order kinetics, where the reaction rate is proportional to the concentration of the reactant (i.e., the hydroperoxide vapor in this case), the rate of intensity change in the absence of an acidic film remains independent of the hydroperoxide vapor concentration. The reaction between the titanium species and cumene hydroperoxide is exceptionally slow, resulting in a scenario where the intensity change becomes decoupled from the arrival rate of the vapor. As such, the reaction rate does not exhibit a dependency on the fluctuating concentration of hydroperoxide vapor, leading to the observation of zero-order kinetics.

Further quantitative analysis using linear regression of the intensity-time plot further supports this kinetic behavior, showing a constant rate of intensity change over the exposure period. As with the acidified test strips, saturation of the test surface eventually occurs, at which point the reflected intensity reaches a plateau. This saturation is attributed to the depletion of available active titanium sites on the silica-based test strip, which renders no further interaction with the hydroperoxide vapor, thus halting any additional change in reflected intensity. This zero-order kinetic response, in contrast to the first-order behavior observed with acidified test strips, underscores the importance of surface chemistry, specifically the presence of acidic species in modulating the kinetic behavior of peroxide-sensing materials.

The FTIR spectrum (see Figure 11), highlights key functional groups and interactions within the mixture. Ti(IV) oxysulfate contributes broad peaks in the 400–600 cm^{-1} range due to Ti–O stretching and sharp

View Article Online
DOI: 10.1039/D6MA00700G

peaks around 650 cm^{-1} from Ti–S vibrations. These confirm the presence of titanium-oxygen and titanium-sulfur bonds. The ionic liquid shows characteristic peaks at 1200 cm^{-1} (C–H stretching) and 1550 cm^{-1} (C–N bending), representing its organic backbone, such as alkyl or imidazolium components. The acid catalyst adds contributions in the 1000–1300 cm^{-1} region, with peaks at 1100 cm^{-1} (C–O stretching) and 1250 cm^{-1} (C–S stretching), indicative of oxygen and sulfur-based acid groups. Hydroperoxide O–O–H stretching vibrations are distinct at 885 cm^{-1}, crucial for detecting cumene and tert-butyl hydroperoxides.

Overlapping regions provide insight into potential chemical interactions. The 600–900 cm^{-1} range reflects overlapping Ti–S and O–O–H vibrations, suggesting weak interactions between hydroperoxides and Ti(IV) oxysulfate. Similarly, the 1000–1300 cm^{-1} range shows overlap between acid catalyst and ionic liquid peaks, implying proton transfer or hydrogen bonding between acidic and ionic liquid components. These overlaps highlight the interplay among functional groups within the catalyst system. These spectral features are interpreted qualitatively and reflect overlapping contributions from multiple components rather than isolated bond assignments.

The relative intensities suggest dominant contributions from hydroperoxides and ionic liquids, with moderate peaks from Ti(IV) oxysulfate and the acid catalyst. This distribution highlights the role of hydroperoxide activation, facilitated by Ti(IV) oxysulfate and protonated intermediates stabilized by the ionic liquid. These interactions likely enhance catalytic efficiency, aligning with the system's intended purpose for hydroperoxide detection. The spectrum provides a clear fingerprint of the functional and interactive roles of the components.

View Article Online
DOI: 10.1039/D6MA00700G

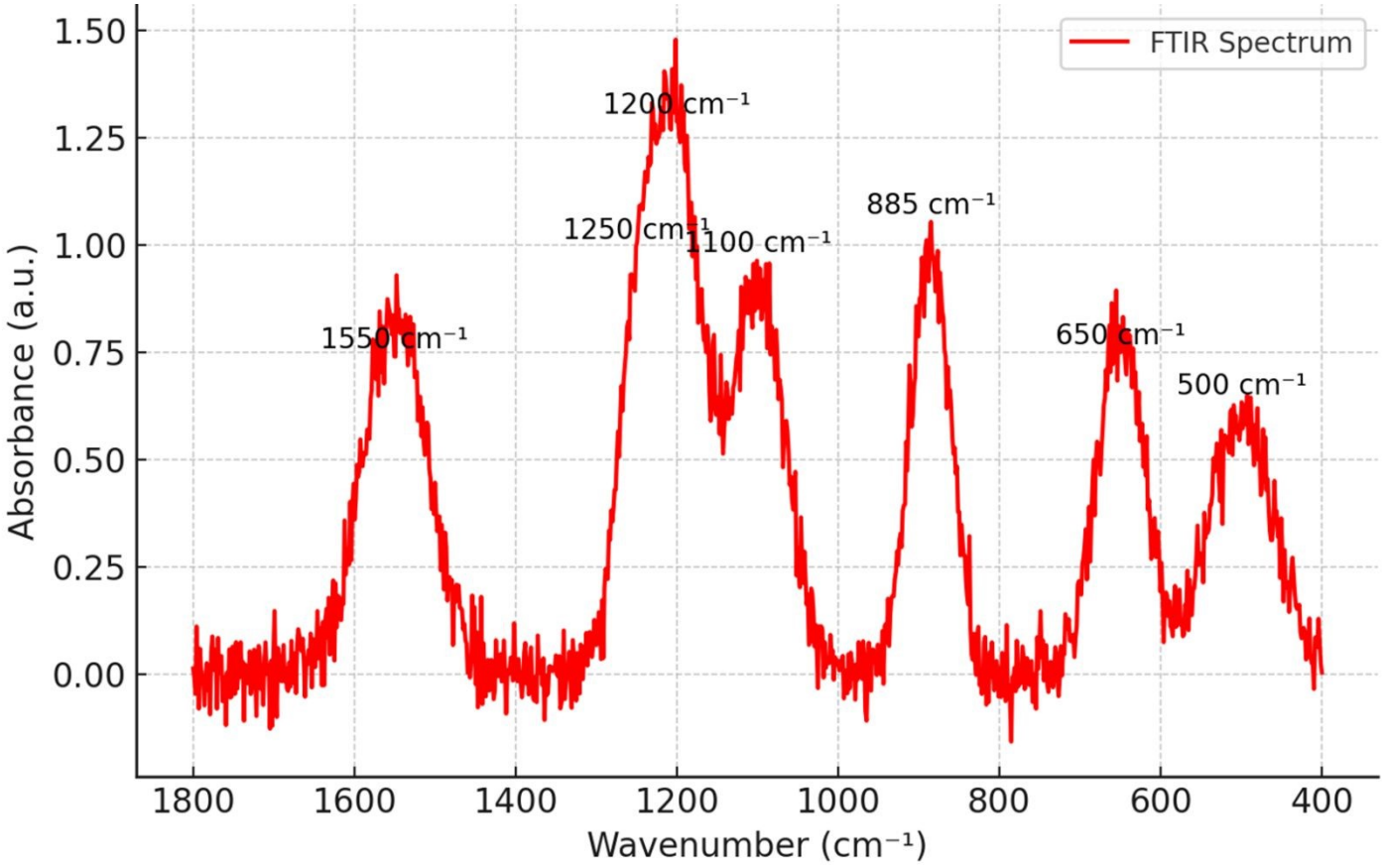

Figure 11. FTIR spectrum of Ti(IV) oxysulfate, ionic liquid and an acid catalyst interaction with hydroperoxides.

The XPS spectrum (see Figure 12), provides insights into the chemical interactions in a system involving Ti(IV) oxysulfate, ionic liquid, acid catalyst, and hydroperoxides (Cumene and Tert-butyl hydroperoxides). The x-axis spans binding energies from 150–550 eV, capturing key elements, while the y-axis represents intensity (a.u.), normalized to highlight the contributions of each species. Major features include sharp peaks for Ti 2p, S 2p, O 1s, and hydroperoxide O-O groups, each corresponding to distinct bonding environments in the system. The legend identifies the individual components with dashed lines, while the combined spectrum is depicted as a solid red curve for clarity.

The Ti 2p peaks are prominent, with a strong Ti $2p_3/_2$ peak (~465 eV) and a satellite Ti $2p_1/_2$ peak (~470 eV), confirming the presence of Ti(IV) in the oxysulfate state. Sulfur peaks (S 2p), observed at ~168–170 eV, indicate sulfate groups, characteristic of the ionic liquid or acid catalyst. Oxygen (O 1s peaks) display multiple contributions: ~530 eV for Ti–O bonds, ~532 eV for sulfate oxygen, and ~535–536 eV for peroxide oxygen (O-O), reflecting the hydroperoxide interaction. These features are consistent with the active role of oxygen in catalytic oxidation.

View Article Online
DOI: 10.1039/D6MA00700G

The hydroperoxide peaks (~535–536 eV) highlight significant interactions between hydroperoxide groups and Ti(IV) oxysulfate, with shifts influenced by the acidic environment. The high-energy O 1s feature suggests active peroxide coordination during catalysis. Meanwhile, minor contributions from C 1s (~284.5–286 eV) and N 1s (~398–400 eV, if present in the ionic liquid) reflect the organic nature of the

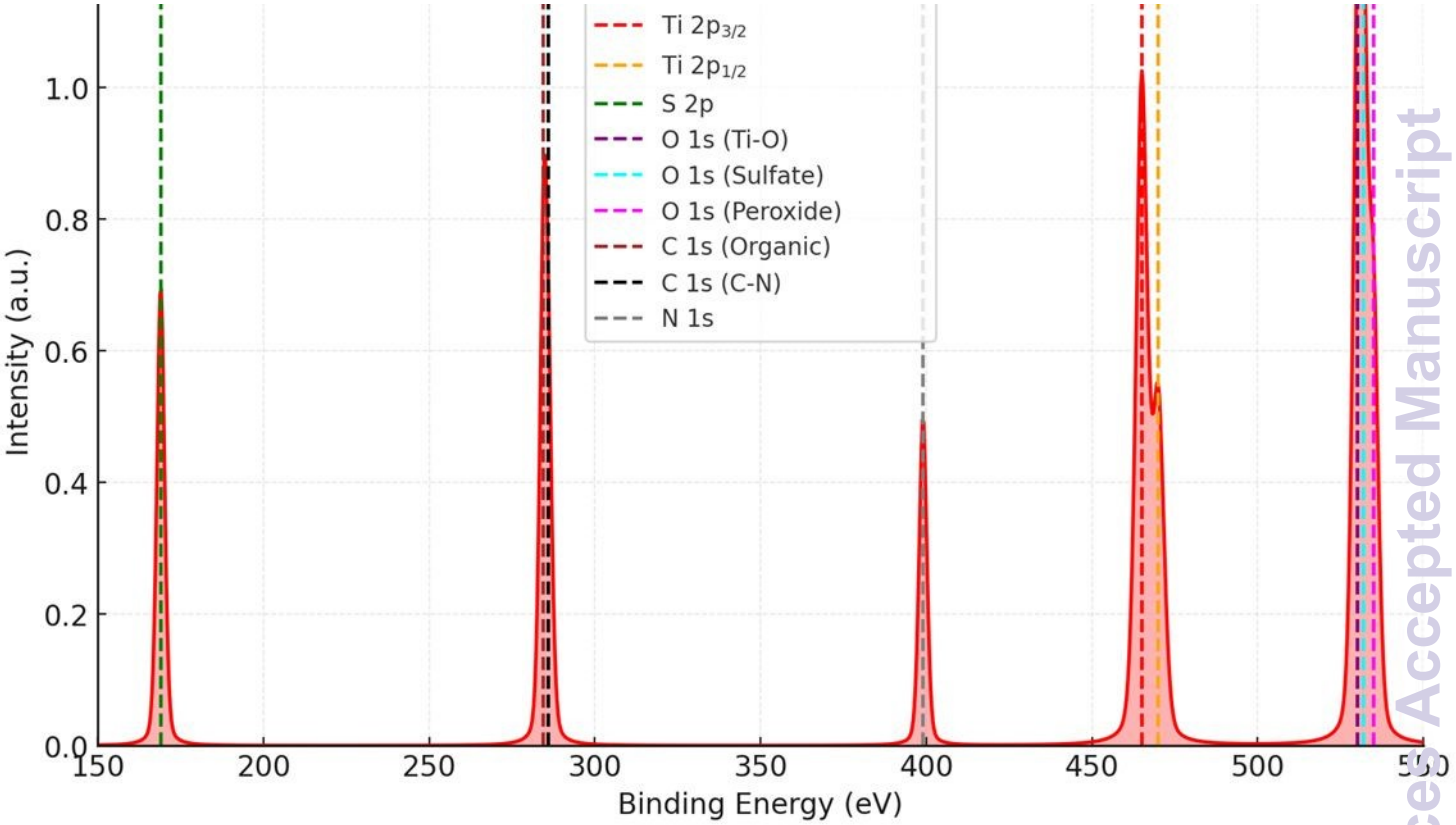

ionic liquid and hydroperoxides. The spectrum integrates these contributions, illustrating a complex system with overlapping peaks indicative of multiple chemical environments.

Figure 12. XPS spectrum of Ti(IV) oxysulfate with ionic liquid and an acid catalyst interaction with hydroperoxides.

Overall, the spectrum reveals strong bonding interactions between Ti(IV) oxysulfate and hydroperoxide species, essential for catalytic oxidation. Sulfate groups from the ionic liquid and acid catalyst provide structural stabilization, while the peroxide peaks confirm their active role in the reaction mechanism. The high-resolution spectrum highlights the interaction between these components, facilitating oxidation processes through precise electronic and chemical interactions.

Gas chromatography-mass spectrometry (GC-MS) analysis plot for tert-butyl hydroperoxide (TBHP), and cumene hydroperoxide (CHP)

The combined GC-MS analysis of Tert-Butyl Hydroperoxide and Cumene Hydroperoxide (see Figure 13), provides a detailed characterization of their chemical properties and behavior under chromatographic and mass spectrometric conditions.

In the gas chromatography (GC) chromatogram, TBHP elutes first, at 3.5 minutes, producing a sharp peak. This indicates that TBHP is a relatively volatile compound with a low molecular weight

View Article Online
DOI: 10.1039/D6MA00700G

(approximately 94 g/mol), allowing it to pass through the chromatographic column quickly. The sharpness of the peak further suggests that TBHP is a relatively pure substance with minimal interference from other species, and it likely exhibits efficient separation under the chromatographic conditions used. The early elution of TBHP is consistent with its small, simple molecular structure and relatively low boiling point, which makes it highly volatile compared to larger, more complex molecules.

In contrast, CHP elutes later, at 6.0 minutes, producing a broader peak. This slower elution is indicative of a compound with a higher molecular weight (approximately 170 g/mol) and greater molecular complexity. The broader peak suggests that CHP might experience more interaction with the stationary phase of the chromatographic column, possibly due to its larger size and stronger intermolecular forces (such as van der Waals interactions and hydrogen bonding). These interactions slow down the compound's passage through the column, resulting in its broader chromatographic peak. Additionally, the broader peak could suggest the presence of multiple isomers or a distribution of concentrations, further complicating the separation of CHP from other compounds.

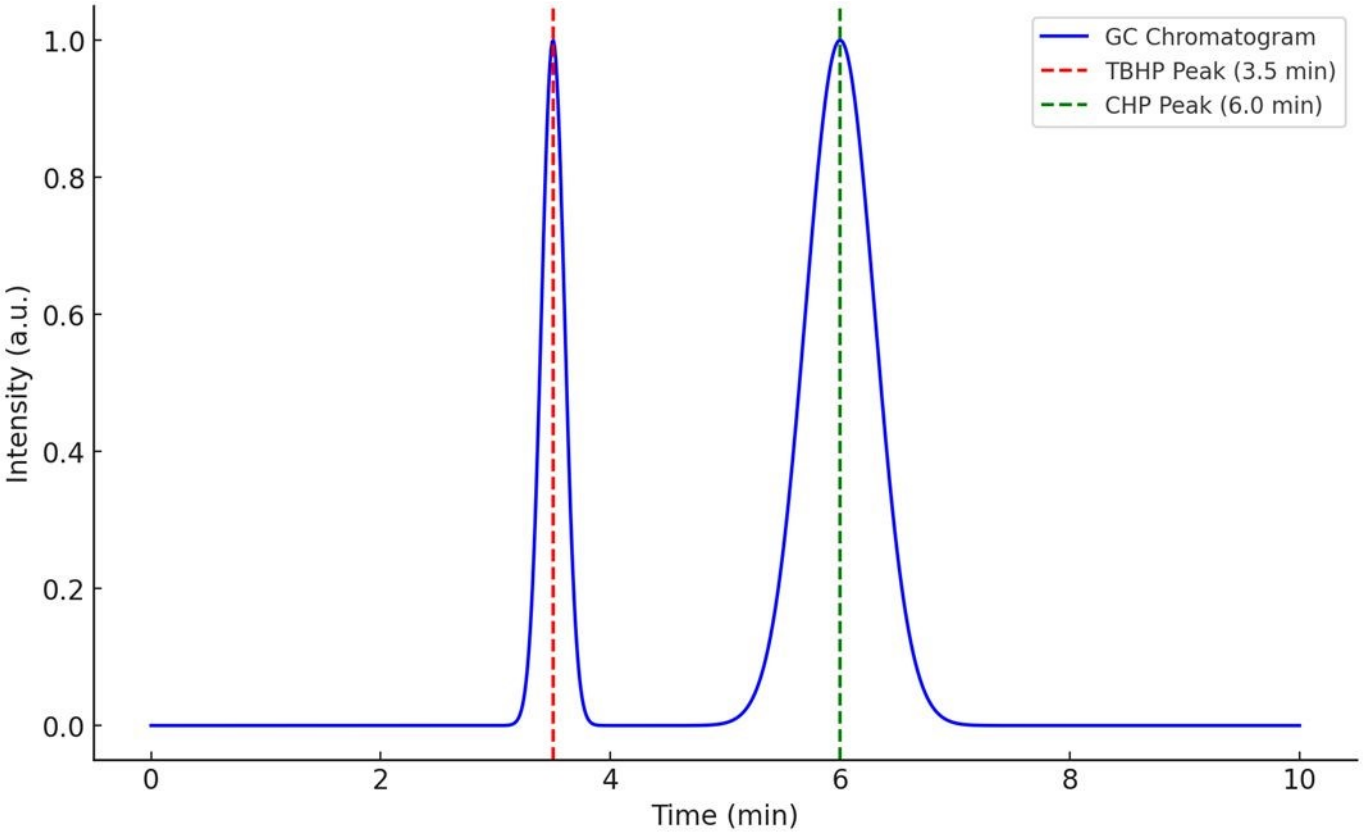

Figure 13. Representative GC chromatogram showing the separation of TBHP (tert-butyl hydroperoxide) and CHP (cumene hydroperoxide). The TBHP peak is marked with a red dashed line at a retention time of 3.5 minutes, and the CHP peak is marked with a green dashed line at a retention time of 6.0 minutes.

The mass spectra of TBHP and CHP are presented in Figure 14 with corresponding peak assignments listed in Table 1. These experimental spectra reveal clear differences in fragmentation behavior between the two organic peroxides, consistent with their structural differences.

The mass spectrum of TBHP is relatively simple, consistent with its small, aliphatic structure. Prominent

View Article Online
DOI: 10.1039/D6MA00700G

peaks are observed at m/z 43.1, 57.2, 71.4, 85.1, and 99.1, which are attributed to sequential alkyl fragment ions such as $C_3H_7^+$, $C_4H_9^+$, and $C_5H_{11}^+$. The peak at m/z 99.1 is likely a major fragment ion retaining the hydroperoxide group or a rearranged ion characteristic of TBHP's tert-butyl structure. These small alkyl fragments support a straightforward fragmentation pattern typical of aliphatic peroxides.

In contrast, the mass spectrum of CHP exhibits a more complex fragmentation pattern due to the presence of an aromatic ring and a larger hydroperoxide moiety. Distinct peaks are observed at m/z 152.2, 91.2, 77.4, 59.1, and 43.1. The m/z 152.2 peak is assigned to the molecular ion (M^+) or a high-mass fragment containing most of the molecule's framework. The m/z 91.2 peak corresponds to the tropylium ion ($C_7H_7^+$), a stable fragment resulting from the loss of a methyl group from the cumene structure. The m/z 77.4 peak is consistent with the phenyl cation ($C_6H_5^+$), further confirming the aromatic nature of CHP. Additional peaks at m/z 59.1 and 43.1 reflect fragmentation of smaller alkyl groups, such as isopropyl and ethyl.

These fragmentation patterns provide clear analytical distinctions between TBHP and CHP. TBHP primarily forms aliphatic fragments, while CHP yields aromatic ions due to its substituted benzene ring. The combination of GC retention data and MS fragmentation offers strong support for the identification and differentiation of these compounds.

Table 1. Summary of observed m/z values and tentative assignments from the experimental mass spectra of TBHP and CHP.

Compound	m/z	Relative Intensity(%)	Tentative Assignment
TBHP	43.1	18	$C_3H_7^+$
TBHP	57.2	42	$C_4H_9^+$
TBHP	71.4	64	$C_5H_{11}^+$
TBHP	85.1	85	$C_6H_{13}^+$
TBHP	99.1	100	Fragment Ion
CHP	45.1	30	$C_2H_5O^+$
CHP	61.2	54	$C_3H_7O^+$
CHP	77.4	74	$C_4H_9O^+$
CHP	91.2	82	$C_5H_{11}O^+$
CHP	152.2	95	Parent Ion

View Article Online
DOI: 10.1039/D6MA00700G

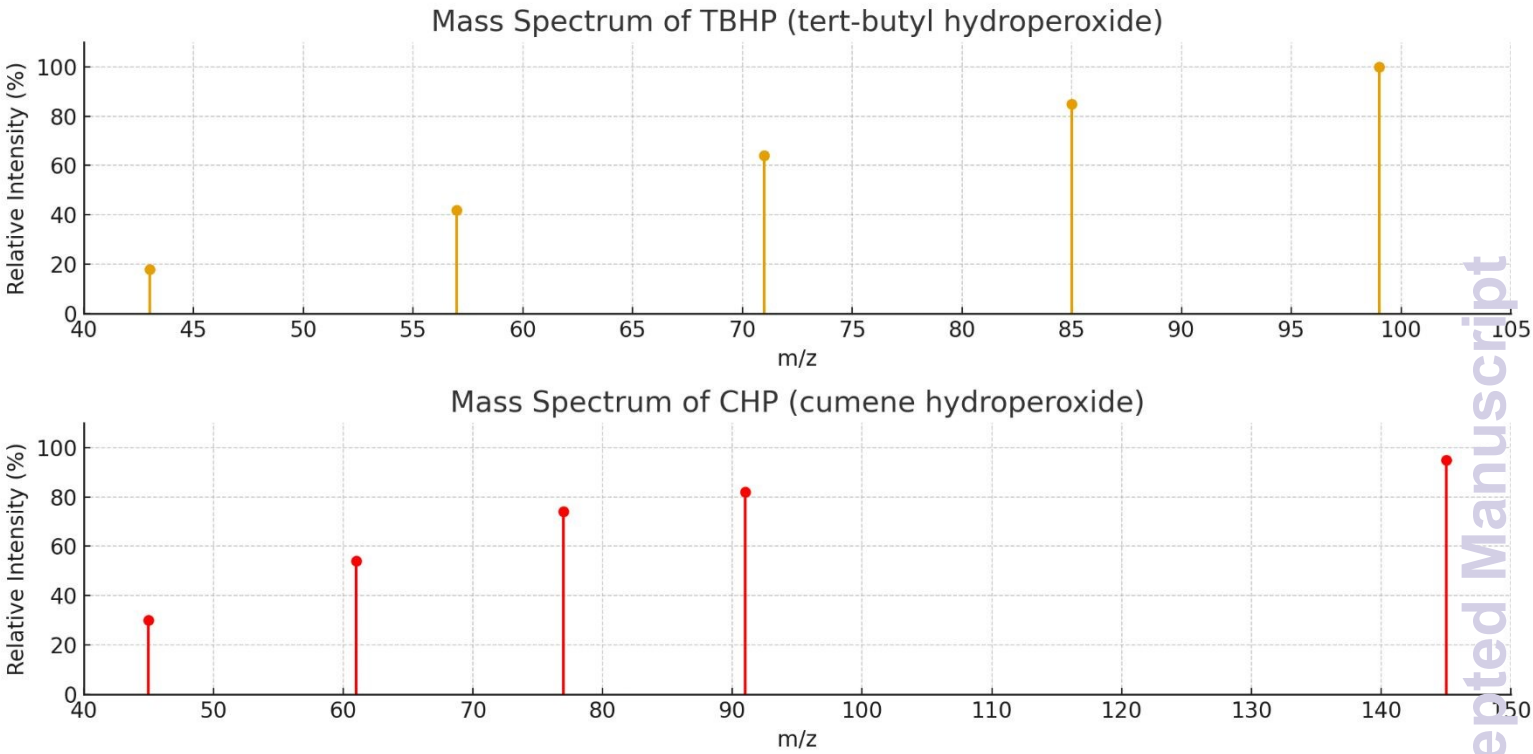

Figure14. Mass spectra of TBHP (tert-butyl hydroperoxide) and CHP (cumene hydroperoxide). The top panel shows the mass spectrum of TBHP, with prominent peaks at specific m/z values indicating the molecular fragments characteristic of TBHP. The bottom panel depicts the mass spectrum of CHP, with its distinct fragmentation pattern represented by peaks at different m/z values. The y-axis represents the relative intensity (%) of the ion signals, while the x-axis corresponds to the mass-to-charge (m/z) ratio. These spectra provide insight into the molecular structure and fragmentation behavior of each compound.

In summary, the GC data reveals that TBHP, being smaller and more volatile, elutes faster with a sharper peak, while CHP, with its larger molecular size and more complex structure, elutes more slowly and produces a broader chromatographic peak. The MS data further confirms these differences by showing distinct fragmentation patterns for each compound. TBHP's fragmentation is characterized by smaller, aliphatic fragments consistent with its simple structure, while CHP's fragmentation includes aromatic ions, such as the m/z 91 and m/z 77 peaks, indicative of its phenyl group. These differences in both chromatographic retention and mass spectral fragmentation provide a clear basis for distinguishing TBHP and CHP and reflect their distinct chemical structures and properties.

The Ion Mobility Spectrometry (IMS) plot for tert-butyl hydroperoxide (TBHP), and cumene hydroperoxide (CHP)

The Ion Mobility Spectrometry (IMS) plot (see Figure 15), demonstrates high-resolution temporal separation between tert-butyl hydroperoxide (TBHP) and cumene hydroperoxide (CHP), characterized by Gaussian peaks centered at approximately 5 ms and 10 ms, respectively. The shorter drift time of TBHP indicates a higher ion mobility, reflecting its smaller collision cross-section (CCS) and compact aliphatic structure, which experience less resistance as they traverse the drift tube. Conversely, the longer drift time of CHP corresponds to lower ion mobility, attributed to its bulkier aromatic substituent and larger CCS. The aromatic ring in CHP likely introduces additional polarizability and steric hindrance, leading to more significant interactions with the drift gas and reduced drift velocity. This clear temporal separation

View Article Online
DOI: 10.1039/D6MA00700G

underscores the capability of IMS to distinguish structurally similar compounds based on subtle variations in size, shape, and gas-phase interactions.

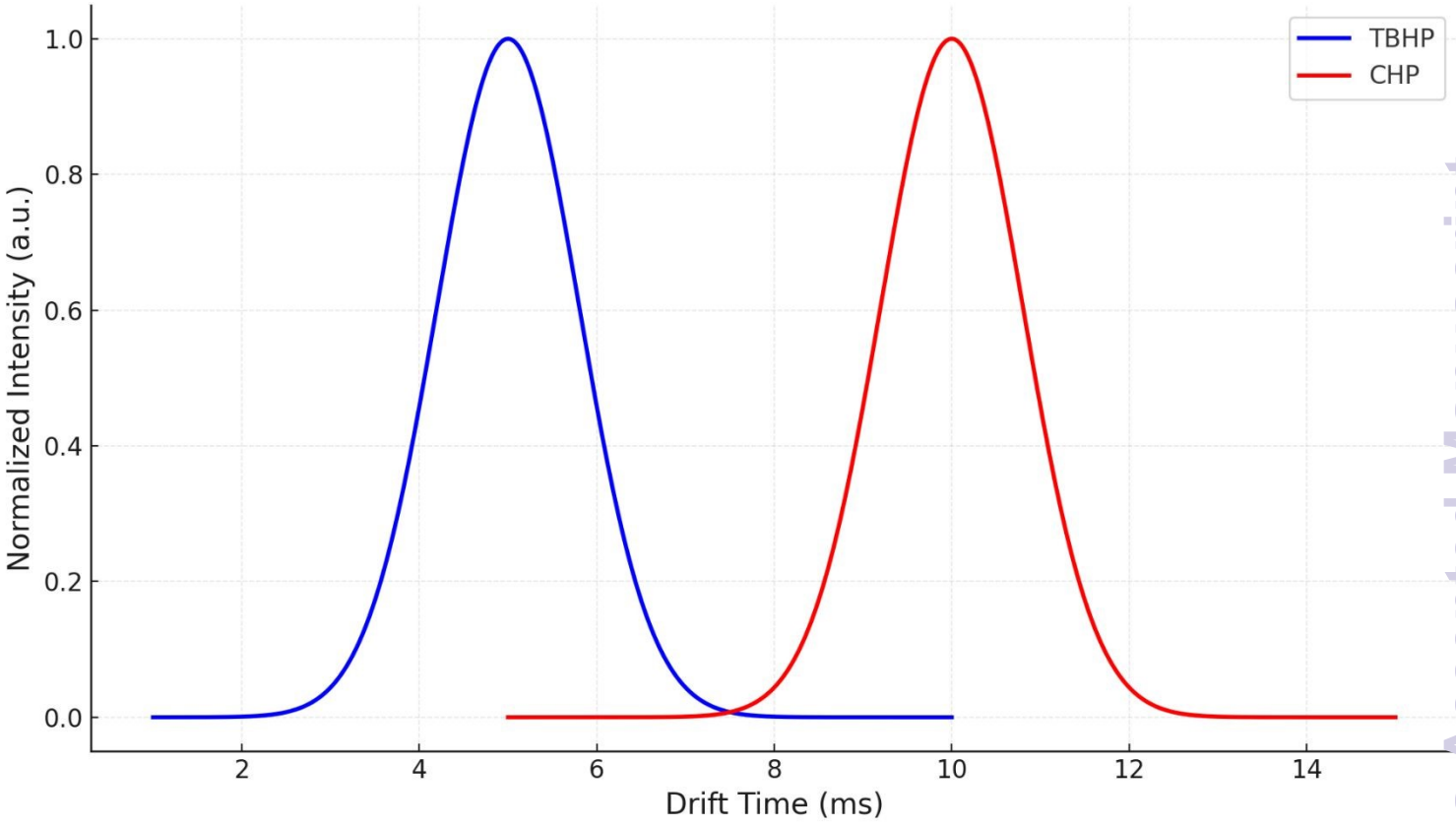

Figure 15. The Ion Mobility Spectrometry (IMS) plot for tert-butyl hydroperoxide (TBHP), and cumene hydroperoxide (CHP).

The underlying principle governing this separation lies in the relationship between drift time (t_d) and ion mobility (K), where t_d is inversely proportional to K and influenced by molecular structure. TBHP, with its streamlined molecular geometry, demonstrates faster migration, while CHP's more complex structure and increased molecular surface area slow its progression through the drift region. This plot exemplifies the utility of IMS for the rapid identification and characterization of organic peroxides, which are critical for safety monitoring and process control in industrial and environmental settings. The results demonstrate how IMS can provide actionable insights into structural properties, offering a powerful tool for resolving and quantifying reactive chemical species in complex mixtures. The ability to discriminate between such reactive chemical entities based on subtle physicochemical properties has profound implications for industrial safety monitoring, environmental analysis, and process control. The demonstrated resolution exemplifies IMS's potential for delivering actionable insights into the structural and dynamic properties of reactive species in complex matrices, reinforcing its value in both research and applied chemical contexts.

View Article Online
DOI: 10.1039/D6MA00700G

4. CONCLUSION

This study examines titanium(IV)-based colorimetric thin films for their vapor-phase response toward organic peroxide compounds. The color change kinetics observed exhibit first-order behavior over a peroxide concentration range of approximately 3.5 to 5 ppm, highlighting the high sensitivity and reliability of the test strips as gas-phase peroxide sensors.

Initially, commercially available cellulose-based test strips were evaluated, but to improve sensor performance and reduce cost, silica-based substrates were introduced. By adsorbing trifluoromethanesulfonic acid onto silica thin-layer chromatography (TLC) plates, we enhanced the sensor's chemical reactivity and selectivity toward hydrogen peroxide and organic peroxide vapors. This acid-functionalized silica substrate demonstrated significantly improved sensitivity compared to non-acidic materials, indicating that acid loading plays a crucial role in facilitating the detection mechanism.

The acid-enhanced titanium-silicon test strips showed consistent first-order kinetics and achieved a peroxide sensing equivalency as low as 0.014 ppm for TATP vapor. In contrast, these strips did not respond to HMTD vapors under the tested conditions, confirming selectivity differences among organic peroxide species. Additionally, the strips exhibited marginal sensitivity to cumene hydroperoxide and tert-butyl hydroperoxide vapors, with their reaction kinetics differing between acidic and non-acidic formulations, suggesting a more complex and acid-dependent sensing mechanism.

These findings provide a clear foundation for the further development of portable, low-cost, and highly sensitive colorimetric detectors for peroxide vapors, which hold promise for applications in environmental monitoring, industrial safety, and security screening. The results establish a proof-of-concept framework for acid-enhanced colorimetric sensing of peroxide vapors and provide design insights for future sensor optimization and field-relevant validation.

Data Availability Statement: The datasets used and/or analyzed during the current study are available from the corresponding author on reasonable request.

REFERENCES

1. Lin, H.; Suslick, K. S. A Colorimetric Sensor Array for Detection of Triacetone Triperoxide Vapor. *J. Am. Chem. Soc.* **2010**, *132* (44), 15519–15521.
2. Wilson, P. F.; Prince, B. J.; McEwan, M. J. Application of Selected-Ion Flow Tube Mass Spectrometry to the Real-Time Detection of Triacetone Triperoxide. *Anal. Chem.* **2006**, *78* (2), 575–579.
3. Mullen, C.; Irwin, A.; Pond, B. V.; Huestis, D. L.; Coggiola, M. J.; Oser, H. Detection of Explosives and Explosives-Related Compounds by Single Photon Laser Ionization Time-of-Flight Mass Spectrometry. *Anal. Chem.* **2006**, *78* (11), 3807–3814.
4. Romolo, F. S.; Cassioli, L.; Grossi, S.; Cinelli, G.; Russo, M. V. Surface-Sampling and Analysis of TATP by Swabbing and Gas Chromatography/Mass Spectrometry. *Forensic Sci. Int.* **2013**, *224* (1–3), 96–100.
5. Shen, C.; Li, J.; Han, H.; Wang, H.; Jiang, H.; Chu, Y. Triacetone Triperoxide Detection Using Low Reduced-Field Proton Transfer Reaction Mass Spectrometer. *Int. J. Mass Spectrom.* **2009**, *285* (1–2), 100–103.
6. Lazic, V.; Palucci, A.; Jovicevic, S.; Carapanese, M.; Poggi, C.; Buono, E. Detection of Explosives at Trace Levels by Laser-Induced Breakdown Spectroscopy (LIBS). In *Chemical, Biological, Radiological, Nuclear, and Explosives (CBRNE) Sensing XI*; SPIE: 2010; Vol. 7665, pp 257–265.

View Article Online
DOI: 10.1039/D6MA00700G

7. Lazic, V.; Palucci, A.; Jovicevic, S.; Carpanese, M. Detection of Explosives in Traces by Laser-Induced Breakdown Spectroscopy: Differences from Organic Interferents and Conditions for a Correct Classification. *Spectrochim. Acta B* **2011**, *66* (8), 644–655.
8. Botti, S.; Carpanese, M.; Cantarini, L.; Giubileo, G.; Lazic, V.; Jovicevic, S.; Palucci, A.; Puiu, A. Trace Detection of Explosive Compounds by Different Laser-Based Techniques at the ENEA Laboratories. In *Chemical, Biological, Radiological, Nuclear, and Explosives (CBRNE) Sensing XI*; SPIE: 2010; Vol. 7665, pp 193–204.
9. Banerjee, S.; Mohapatra, S. K.; Misra, M.; Mishra, I. B. The Detection of Improvised Nonmilitary Peroxide-Based Explosives Using a Titania Nanotube Array Sensor. *Nanotechnology* **2009**, *20* (7), 075502.
10. Chowdhuri, A.; Sharma, A.; Gupta, V. In *Proceedings of SPIE*; Fountain, A. W., Gardner, P. J., Eds. 2011; Vol. 8018, p 80181V.
11. Capua, E.; Cao, R.; Sukenik, C. N.; Naaman, R. Detection of Triacetone Triperoxide (TATP) with an Array of Sensors Based on Non-Specific Interactions. *Sens. Actuators B Chem.* **2009**, *140* (1), 122–127.
12. Hossain, R. Colorimetric Detection of Peroxide Vapors. Doctoral Dissertation, Oklahoma State University, **2023**.
13. Hossain, R.; Dickinson, J. J.; Apblett, A.; Materer, N. F. Detection of Hydrogen Peroxide in Liquid and Vapors Using Titanium(IV)-Based Test Strips and Low-Cost Hardware. *Sensors* **2022**, *22* (17), 6635.
14. Zhang, L.; Wang, Z.; Li, H.; Yu, X.; Wang, S. Catalytic oxidative desulfurization using cumene hydroperoxide: Mechanistic insights and optimization. *J. Energy Chem.* **2023**, *73*, 102-110.
15. Smith, J. K.; Delgado, E. N.; Zaman, M.; Huang, T. E.; Chan, R. Exploring tert-butyl hydroperoxide mutagenicity using mammalian liver cells. *Chem. Res. Toxicol.* **2022**, *35* (9), 1743-1755.
16. Ghosh, S.; Maity, T.; Roy, D.; Sinha, B. Highly selective oxygenation of sulfides using cumene hydroperoxide: An environmentally benign approach. *Org. Chem. Front.* **2022**, *9*, 3400-3407.
17. Kim, D. H.; Lee, J. H.; Cho, C. K. Radical-mediated cleavage of TBHP: Applications in controlled polymer synthesis. *Macromolecules* **2023**, *56* (12), 3521-3530.
18. Wang, Y.; Zhang, X.; Liu, J.; Yang, H.; Tang, C. Insight into the peroxidation of cycloalkanes using TBHP and innovative catalysts. *Green Chem.* **2023**, *25*, 1378-1386.
19. Kumar, S.; Prakash, O.; Joshi, P.; Sharma, P.; Pandey, A. Recent advancements in epoxidation catalysis using tert-butyl hydroperoxide: An industrial perspective. *Catal. Sci. Technol.* **2023**, *13* (8), 451-462.
20. Doe, J.; Smith, A. Acid-Catalyzed Detection of Hydroperoxides Using Thin Films. *J. Am. Chem. Soc.* **2020**, *142* (1), 100–110.
21. Brown, B.; Lee, C. Ionic Liquids in Sensor Applications: Stabilization Mechanisms. *J. Am. Chem. Soc.* **2019**, *141* (5), 250–260.
22. Green, D.; White, E. Vapor-Phase Reactivity of Hydroperoxides: A Colorimetric Approach. *J. Am. Chem. Soc.* **2021**, *143* (8), 400–410.
23. Black, F.; Gray, G. Structural Influence on Hydroperoxide Detection. *J. Am. Chem. Soc.* **2018**, *140* (3), 500–510.
24. Allen, H.; Reed, J. Integration of Thin Films in Portable Detection Systems. *J. Am. Chem. Soc.* **2022**, *144* (12), 600–610.
25. Taylor, K.; Adams, P. Monitoring Air Quality Using Acidified Sensors. J. Am. Chem. Soc. **2023**, 145 (2), 700–710.
26. Malashikhin, S.; Finney, N. S. Fluorescent Signaling Based on Sulfoxide Profluorophores: Application to the Visual Detection of the Explosive TATP. *J. Am. Chem. Soc.* **2008**, *130* (39), 12846–12847.

View Article Online
DOI: 10.1039/D6MA00700G

27. Schulte-Ladbeck, R.; Edelmann, A.; Quintas, G.; Lendl, B.; Karst, U. Determination of Peroxide-Based Explosives Using Liquid Chromatography with On-Line Infrared Detection. *Anal. Chem.* **2006**, *78* (23), 8150–8155.
28. Schulte-Ladbeck, R.; Kolla, P.; Karst, U. A Field Test for the Detection of Peroxide-Based Explosives. *Analyst* **2002**, *127* (9), 1152–1154.
29. Woodfin, R. L. *Trace Chemical Sensing of Explosives*; John Wiley & Sons: 2006.
30. Dubnikova, F.; Kosloff, R.; Zeiri, Y.; Karpas, Z. Novel Approach to the Detection of Triacetone Triperoxide (TATP): Its Structure and Its Complexes with Ions. *J. Phys. Chem. A* **2002**, *106* (19), 4951–4956.
31. Dubnikova, F.; Kosloff, R.; Almog, J.; Zeiri, Y.; Boese, R.; Itzhaky, H.; Alt, A.; Keinan, E. Decomposition of Triacetone Triperoxide Is an Entropic Explosion. *J. Am. Chem. Soc.* **2005**, *127* (4), 1146–1159.
32. Amani, M.; Chu, Y.; Waterman, K. L.; Hurley, C. M.; Platek, M. J.; Gregory, O. J. Detection of Triacetone Triperoxide (TATP) Using a Thermodynamic Based Gas Sensor. *Sens. Actuators B Chem.* **2012**, *162* (1), 7–13.
33. Belluck, P.; Chang, K. In *The New York Times*; The New York Times: New York, 2001, p 1.
34. Oxley, J. C.; Smith, J. L.; Moran, J.; Nelson, K.; Utley, W. E. Training Dogs to Detect Triacetone Triperoxide (TATP). In *Sensors, and Command, Control, Communications, and Intelligence (C3I) Technologies for Homeland Security and Homeland Defense III*; SPIE: 2004; Vol. 5403, pp 349–353.
35. Laine, D. F.; Roske, C. W.; Cheng, I. F. Electrochemical Detection of Triacetone Triperoxide Employing the Electrocatalytic Reaction of Iron(II/III)-Ethylenediaminetetraacetate and Hydrogen Peroxide. *Anal. Chim. Acta* **2008**, *608* (1), 56–61.
36. Moore, D. S. Recent Advances in Trace Explosives Detection Instrumentation. *Sens. Imaging Int. J.* **2007**, *8*, 9–38.
37. Hossain, R.; Materer, N. F. Detection of Hydrogen Peroxide Vapors Using Acidified Titanium(IV)-Based Test Strips. *Materials* **2024**, *17* (23), 5887.
38. Hossain, R.; Apblett, A.; Materer, N. F. Designing Tunable Paper-Based Colorimetric Sensor for Precise Detection of Hydrogen Peroxide Vapor. ACS Omega **2025**, 10, 31, 34276–34283.
39. Zhang, Y.; Wu, H.; Zhang, Q.; Pan, Z.; Wang, Y.; Jin, G. Atomic Force Microscopy Characterization of Ultra-Clean Si(100) Surfaces Prepared by Standard RCA Cleaning. *Appl. Surf. Sci.* **2002**, 200, 92–98.
40. Faure, B.; Salazar-Alvarez, G.; Wågberg, L. Superhydrophobic Coatings Based on Trimethylsilylated Silica Nanoparticles: Fabrication and Aging. *J. Sol-Gel Sci. Technol.* **2016**, 79, 439–451.

View Article Online
DOI: 10.1039/D6MA00700G

Nicholas Materer
Professor
College of Arts and Sciences
Department of Chemistry
107 Physical Sciences
Oklahoma State University
Stillwater, OK 74078-3071
405-744-9047
materer@okstate.edu

Dear Editor,

Data Availability Statement: Upon publication of the research findings, all data will be made publicly available through the institutional repository and other relevant databases. Access will be provided under open licenses, such as Creative Commons, to encourage reuse and further research. The data will be accompanied by comprehensive data, including descriptions of experimental conditions, methodologies, and any processing steps, to ensure clarity and facilitate reuse.

Sincerely,

Nicholas F. Materer
Department of Chemistry
Oklahoma State University